

Cationic Polymerization and Insertion Chemistry in the Reactions of Vinyl Ethers with (α -Diimine) PdMe^+ Species

Changle Chen, Shuji Luo, and Richard F. Jordan*

Department of Chemistry, The University of Chicago, 5735 South Ellis Avenue,
Chicago, Illinois 60637

Received January 19, 2010; E-mail: rfjordan@uchicago.edu

Abstract: The reactions of (α -diimine) PdMe^+ species (**1**, α -diimine = (2,6- $\text{tPr}_2\text{-C}_6\text{H}_3$) $\text{N}=\text{CMeCMe}=\text{N}$ (2,6- $\text{tPr}_2\text{-C}_6\text{H}_3$)) with vinyl ethers $\text{CH}_2=\text{CHOR}$ (**2a–g**; **R** = tBu (**a**), Et (**b**), SiMe_3 (**c**), SiMe_2Ph (**d**), SiMePh_2 (**e**), SiPh_3 (**f**), Ph (**g**); **2a–g**; **R** = tBu (**a**), Et (**b**), SiMe_3 (**c**), SiMe_2Ph (**d**), SiMePh_2 (**e**), SiPh_3 (**f**), Ph (**g**)) were investigated. Two pathways were observed. First, **1** initiates the cationic polymerization of **2a–c** with concomitant decomposition of **1** to Pd^0 . This reaction proceeds by formation of (α -diimine) $\text{PdR}'(\text{CH}_2=\text{CHOR})^+ \pi$ complexes ($\text{R}' = \text{Me}$ or CH_2CHMeOR from insertion), in which the vinyl ether $\text{C}=\text{C}$ bond is polarized with carbocation character at the substituted carbon (C_{int}). Electrophilic attack of C_{int} on monomer initiates polymerization. Second, **1** reacts with stoichiometric quantities of **2a–g** by formation of (α -diimine) $\text{PdMe}(\text{CH}_2=\text{CHOR})^+$ (**3a–g**), insertion to form (α -diimine) $\text{Pd}(\text{CH}_2\text{CHMeOR})^+$ (**4a–g**), reversible isomerization to (α -diimine) $\text{Pd}(\text{CMe}_2\text{OR})^+$ (**5a–g**), β -OR elimination of **4a–g** to generate (α -diimine) $\text{Pd}(\text{OR})(\text{CH}_2=\text{CHMe})^+$ (not observed), and allylic $\text{C}-\text{H}$ activation to yield (α -diimine) $\text{Pd}(\eta^3\text{-C}_3\text{H}_5)^+$ (**6**) and ROH . Binding strengths vary in the order **2a** > **2b** ~ **2c** > **2d** ~ **2g** > **2e** > **2f**. Strongly electron-donating OR groups increase the binding strength, while steric crowding has the opposite effect. The insertion rates vary in the order **3a** < **3b** < **3c** < **3d** < **3e** < **3f** < **3g**; this trend is determined primarily by the relative ground-state energies of **3a–g**. The β -OR elimination rates vary in the order O^iBu < OSiR_3 < OPh . For **2d–g**, the insertion chemistry out-competes cationic polymerization even at high vinyl ether concentrations. β -OR elimination of **4/5** mixtures is faster for SbF_6^- salts than $\text{B}(\text{C}_6\text{F}_5)_4^-$ salts. The implications of these results for olefin/vinyl ether copolymerization are discussed.

Introduction

The development of catalysts that are capable of polymerizing or copolymerizing functionalized vinyl monomers ($\text{CH}_2=\text{CHX}$) by insertion mechanisms would enable the synthesis of new polyolefins with enhanced properties.¹ The discovery by Brookhart and co-workers that (α -diimine) PdR^+ catalysts copolymerize ethylene and acrylate monomers to highly branched copolymers was a seminal development in this field.² More recently, several groups have shown that (*ortho*-phosphino-arenesulfonate) PdR catalysts copolymerize ethylene with acrylates, vinyl ethers, vinyl fluoride, acrylonitrile, vinyl acetate, and other comonomers to linear copolymers.³ However, in other cases, it has been found that $\text{CH}_2=\text{CHX}$ monomers deactivate olefin polymerization catalysts. Several common deactivation processes have been

identified, including (i) coordination of the $\text{CH}_2=\text{CHX}$ monomer to the L_nMR^+ active species through the X group rather than the $\text{C}=\text{C}$ bond to form unreactive $\text{L}_n\text{MR}(\kappa\text{-X-XCH}=\text{CH}_2)^+$ adducts;⁴ (ii) formation of $\text{L}_n\text{MCH(X)CH}_2\text{R}$ species that are resistant to subsequent insertion reactions due to X chelation, which blocks the site required for monomer coordination,⁵ and the electronic influence of the X substituent;⁶ and (iii) β -X elimination of $\text{L}_n\text{MCH}_2\text{CHXR}$ or $\text{L}_n\text{MCHRCH}_2\text{X}$ species to form unreactive L_nMX species.⁷ Moreover, metal catalysts can

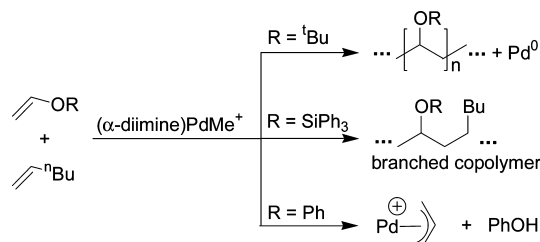
- (1) (a) Boffa, L. S.; Novak, B. M. *Chem. Rev.* **2000**, *100*, 1479. (b) Dong, J. Y.; Hu, Y. L. *Coord. Chem. Rev.* **2006**, *250*, 47. (c) Drent, E.; Budzelaar, P. H. M. *Chem. Rev.* **1996**, *96*, 663. (d) Müller, C.; Rieger, B. *Prog. Polym. Sci.* **2002**, *27*, 815. (e) Chung, T. C. *Prog. Polym. Sci.* **2002**, *27*, 39. (f) Ittel, S. D.; Johnson, L. K.; Brookhart, M. *Chem. Rev.* **2000**, *100*, 1169. (g) Sen, A. *Pure Appl. Chem.* **2001**, *73*, 251. (h) Chen, E. Y. X. *Chem. Rev.* **2009**, *109*, 5157. (i) Nakamura, A.; Ito, S.; Nozaki, K. *Chem. Rev.* **2009**, *109*, 5215. (2) (a) Leatherman, M. D.; Svejda, S. A.; Johnson, L. K.; Brookhart, M. *J. Am. Chem. Soc.* **2003**, *125*, 3068. (b) Shultz, L. H.; Tempel, D. J.; Brookhart, M. *J. Am. Chem. Soc.* **2001**, *123*, 11539. (c) Gottfried, A. C.; Brookhart, M. *Macromolecules* **2001**, *34*, 1140. (d) Tempel, D. J.; Johnson, L. K.; Huff, R. L.; White, P. S.; Brookhart, M. *J. Am. Chem. Soc.* **2000**, *122*, 6686. (e) Johnson, L. K.; Killian, C. M.; Brookhart, M. *J. Am. Chem. Soc.* **1995**, *117*, 6414.

- (3) (a) Drent, E.; van Dijk, R.; van Ginkel, R.; van Oort, B.; Pugh, R. I. *Chem. Commun.* **2002**, 964. (b) Vela, J.; Lief, G. R.; Shen, Z.; Jordan, R. F. *Organometallics* **2007**, *26*, 6624. (c) Guironnet, D.; Roesle, P.; Runzi, T.; Gottker-Schnetmann, I.; Mecking, S. *J. Am. Chem. Soc.* **2009**, *131*, 422. (d) Kochi, T.; Noda, S.; Yoshimura, K.; Nozaki, K. *J. Am. Chem. Soc.* **2007**, *129*, 8948. (e) Luo, S.; Vela, J.; Lief, G. R.; Jordan, R. F. *J. Am. Chem. Soc.* **2007**, *129*, 8946. (f) Weng, W.; Shen, Z.; Jordan, R. F. *J. Am. Chem. Soc.* **2007**, *129*, 15450. (g) Ito, S.; Munakata, K.; Nakamura, A.; Nozaki, K. *J. Am. Chem. Soc.* **2009**, *131*, 14606. (h) Skupov, K. M.; Marella, P. R.; Simard, M.; Yap, G. P. A.; Allen, N.; Conner, D.; Goodall, B. L.; Claverie, J. P. *Macromol. Rapid Commun.* **2007**, *28*, 2033. (i) Skupov, K. M.; Piche, L.; Claverie, J. P. *Macromolecules* **2008**, *41*, 2309. (j) Newsham, D. K.; Borkar, S.; Sen, A.; Conner, D. M.; Goodall, B. L. *Organometallics* **2007**, *26*, 3636. (4) (a) Wu, F.; Foley, S. R.; Burns, C. T.; Jordan, R. F. *J. Am. Chem. Soc.* **2005**, *127*, 1841. (b) Wu, F.; Jordan, R. F. *Organometallics* **2006**, *25*, 5631. (c) Yang, S.-Y.; Szabo, M. J.; Michalak, A.; Weiss, T.; Piers, W. E.; Jordan, R. F.; Ziegler, T. *Organometallics* **2005**, *24*, 1242. (5) Williams, B. S.; Leatherman, M. D.; White, P. S.; Brookhart, M. *J. Am. Chem. Soc.* **2005**, *127*, 5132.

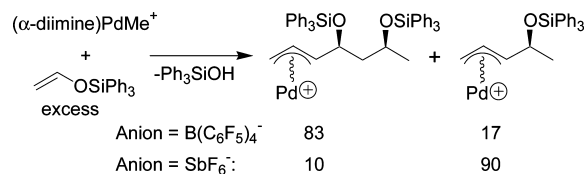
initiate undesired radical or ionic homopolymerization of $\text{CH}_2=\text{CHX}$ monomers.^{8,9}

Vinyl ethers ($\text{CH}_2=\text{CHOR}$) are attractive candidates for insertion copolymerization with olefins because their steric and electronic properties can be tuned by varying the R group, possibly enabling the deactivation reactions noted above to be avoided. Several potential problems can be anticipated for vinyl ethers in insertion polymerization. First, vinyl ethers are highly susceptible to cationic polymerization,¹⁰ and electrophilic olefin polymerization catalysts are good cationic initiators.^{11,12} For example, $[(\text{P}\sim\text{N})\text{PdMe}(\text{CH}_3\text{CN})][\text{BF}_4]$ ($\text{P}\sim\text{N} = o\text{-C}_6\text{H}_4(\text{PPh}_2)\text{-}(\text{N}=\text{CHAr})$, $\text{Ar} = \text{C}_6\text{H}_5$, $4\text{-F-C}_6\text{H}_5$) species initiate cationic polymerization of ethyl vinyl ether to generate poly(ethyl vinyl ether) with a molecular weight of ca. 8000.^{11b} Second, vinyl ethers can coordinate to metals not only through the $\text{C}=\text{C}$ bond, as in $[\text{NEt}_4][\text{PtCl}_3(\text{CH}_2=\text{CHOEt})]^{13}$ and $\text{PdCl}_2[\text{NMe}_2\text{CH}_2\text{-CMe}_2(\text{CH}=\text{CHOMe})]^{14,15}$ but also through the OR group, as in $(\text{C}_5\text{H}_4\text{Me})_2\text{Zr}(\text{O}^t\text{Bu})(\eta^1\text{-O-EtOCH}=\text{CH}_2)^+$ and $\text{RuH}(\text{CO})(\text{P}^t\text{Bu}_2\text{Me})_2(\eta^1\text{-O-EtOCH}=\text{CH}_2)^+.$ ^{15c,16} Third, the insertion barriers for $\text{L}_n\text{MR}'(\text{CH}_2=\text{CHOR})$ species are predicted to be high. For

Scheme 1



Scheme 2



example, the insertion barrier of $(\text{HN}=\text{CHCH}=\text{NH})\text{PdMe}(\text{CH}_2=\text{CHOMe})^+$ was calculated by DFT to be ca. 6 kcal/mol higher than that for $(\text{HN}=\text{CHCH}=\text{NH})\text{PdMe}(\text{CH}_2=\text{CH}_2)^+.$ ¹⁷ Nevertheless, insertions of vinyl ethers into metal hydrides, such as $\text{RuH}(\text{CO})(\text{P}^t\text{Bu}_2\text{Me})_2(\eta^2\text{-CH}_2\text{Cl}_2)^+$, $(\text{Bu}_3\text{SiO})_3\text{TaH}_2$, and $\text{Os}_3\text{H}_2(\text{CO})_{10}$, have been reported.^{16,18,19} Also, $\text{CH}_2=\text{CHOEt}$ inserts into the Pd-acetyl bond of $[(\text{P}\sim\text{N})\text{Pd}(\text{COCH}_3)(\text{CH}_3\text{CN})][\text{BF}_4]$ to generate $[(\text{P}\sim\text{N})\text{Pd-CH}(\text{OEt})\text{CH}_2\text{COCH}_3][\text{BF}_4].$ ^{11b} Finally, $\text{L}_n\text{MCH}_2\text{CH}(\text{OR})\text{R}'$ species formed by 1,2 insertion of $\text{L}_n\text{MR}'(\text{CH}_2=\text{CHOR})$ species may undergo β -OR elimination, which would terminate chain growth. Wolczanski showed that $(\text{Bu}_3\text{SiO})_3\text{TaH}_2$ undergoes 1,2 insertion of $\text{CH}_2=\text{CHOR}$ ($\text{R} = \text{alkyl, Ph}$) to generate $(\text{Bu}_3\text{SiO})_3\text{TaH}(\text{CH}_2\text{CH}_2\text{OR})$ species, which undergo β -OR elimination. However, the β -OR elimination rate decreases as the size of R increases, and $(\text{Bu}_3\text{SiO})_3\text{TaH}(\text{CH}_2\text{CH}_2\text{O}^t\text{Bu})$ is stable.¹⁸

Recently, we reported that $(\alpha\text{-diimine})\text{PdMe}^+$ species ($\alpha\text{-diimine} = (2,6\text{-}i\text{Pr}_2\text{-C}_6\text{H}_3)\text{N}=\text{CMeCMe}=\text{N}(2,6\text{-}i\text{Pr}_2\text{-C}_6\text{H}_3))$ copolymerize 1-hexene and $\text{CH}_2=\text{CHOSiPh}_3$ to OSiPh_3 -substituted polyhexene (Scheme 1).²⁰ Alkyl vinyl ethers such as $\text{CH}_2=\text{CHO}^t\text{Bu}$ are not suitable comonomers in this system due to competing cationic polymerization and Pd^0 formation. Phenyl vinyl ether is also unsuitable because $(\alpha\text{-diimine})\text{Pd}(\text{CH}_2\text{CHMeOPh})^+$ species generated by $\text{CH}_2=\text{CHOPh}$ insertion undergo rapid β -OPh elimination, ultimately forming $(\alpha\text{-diimine})\text{Pd}(\eta^3\text{-C}_3\text{H}_5)^+$, which is catalytically inactive, and PhOH . Further studies showed that $(\alpha\text{-diimine})\text{PdMe}^+$ species undergo up to three sequential insertions of $\text{CH}_2=\text{CHOSiPh}_3$, ultimately forming Pd allyl products (Scheme 2).²¹ The product distribution is dependent on the anion.

In this paper, we describe a comprehensive study of the reactions of $(\alpha\text{-diimine})\text{PdMe}^+$ species with a set of vinyl ethers with varying steric and electronic properties, $\text{CH}_2=\text{CHOR}$ (**2a–g**: $\text{R} = ^t\text{Bu}$ (**a**), Et (**b**), SiMe_3 (**c**), SiMe_2Ph (**d**), SiMePh_2 (**e**), SiPh_3 (**f**), Ph (**g**)). We first describe studies of the reaction of $(\alpha\text{-diimine})\text{PdMe}^+$ with excess **2a–g** to probe the potential

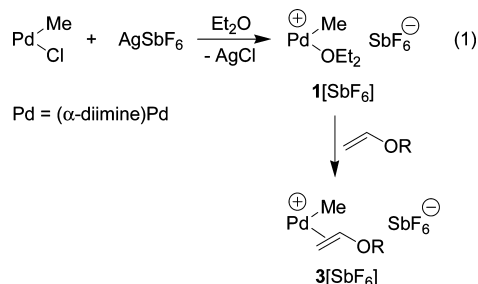
- (6) (a) Foley, S. R.; Shen, H.; Qadeer, U. A.; Jordan, R. F. *Organometallics* **2004**, *23*, 600. (b) Philipp, D. M.; Muller, R. P.; Goddard, W. A.; Storer, J.; McAdon, M.; Mullins, M. *J. Am. Chem. Soc.* **2002**, *124*, 10198. (c) Szabo, M. J.; Jordan, R. F.; Michalak, A.; Piers, W. E.; Weiss, T.; Yang, S.; Ziegler, T. *Organometallics* **2004**, *23*, 5565. (d) Mitoraj, M.; Michalak, A. *J. Mol. Modeling* **2005**, *11*, 341.
- (7) (a) Foley, S. R.; Stockland, R. A.; Shen, H.; Jordan, R. F. *J. Am. Chem. Soc.* **2003**, *125*, 4350. (b) Kang, M.; Sen, A.; Zakharov, L.; Rheingold, A. L. *J. Am. Chem. Soc.* **2002**, *124*, 12080.
- (8) Stockland, R. A.; Foley, S. R.; Jordan, R. F. *J. Am. Chem. Soc.* **2003**, *125*, 796.
- (9) (a) Schaper, F.; Foley, S. R.; Jordan, R. F. *J. Am. Chem. Soc.* **2004**, *126*, 2114. (b) Stojcevic, G.; Prokopchuk, E. M.; Baird, M. C. *J. Organomet. Chem.* **2005**, *690*, 4349.
- (10) (a) Sawamoto, M. *Prog. Polym. Sci.* **1991**, *16*, 111. (b) Kennedy, J. P.; Iva'n, B. *Designed Polymers by Carbocationic Macromolecular Engineering: Theory and Practice*; Hanser: Munich, 1992. (c) Matyjaszewski, K. *Cationic Polymerizations*; Marcel Dekker: New York, 1996. (d) Katayama, H.; Kamigaito, M.; Sawamoto, M. *J. Polym. Sci., Part A: Polym. Chem.* **2001**, *39*, 1249. (e) Higashimura, T.; Sawamoto, M. In *Comprehensive Polymer Science*; Pergamon: Allen, G., Bevington, J., Eds.; Oxford: U.K., 1989; Vol. 3, pp 673–696. Vinyl ethers are poor substrates for radical polymerization. See: (f) Matsumoto, A.; Nakane, T.; Oiwa, M. *Makromol. Chem., Rapid Commun.* **1983**, *4*, 277. (g) Kamachi, M.; Tanaka, K.; Kuwae, Y. *J. Polym. Sci., Part A: Polym. Chem.* **1986**, *24*, 925.
- (11) (a) Baird, M. C. *Chem. Rev.* **2000**, *100*, 1471. (b) Chen, C. L.; Chen, Y. C.; Liu, Y. H.; Peng, S. M.; Liu, S. T. *Organometallics* **2002**, *21*, 5382. (c) Chen, Y. C.; Reddy, K. R.; Liu, S. T. *J. Organomet. Chem.* **2002**, *656*, 199. (d) Albietz, P. J., Jr.; Yang, K.; Lachicotte, R. J.; Eisenberg, R. *Organometallics* **2000**, *19*, 3543. (e) Albietz, P. J., Jr.; Yang, K.; Eisenberg, R. *Organometallics* **1999**, *18*, 2747. (f) Shaffer, T. D.; Ashbaugh, J. R. *J. Polym. Sci., Part A: Polym. Chem.* **1997**, *35*, 329. (g) Kawaguchi, T.; Sanda, F. O.; Masuda, T. *J. Polym. Sci., Part A: Polym. Chem.* **2002**, *40*, 3938.
- (12) For vinyl ether polymerizations mediated by combinations of metal complexes and silanes, see: (a) Nagashima, H.; Itonaga, C.; Yasuhara, J.; Motoyama, Y.; Matsubara, K. *Organometallics* **2004**, *23*, 5779. (b) Crivello, J. V.; Fan, M. *J. Polym. Sci., Part A: Polym. Chem.* **1991**, *29*, 1853.
- (13) Elder, R. C.; Pesa, F. *Acta Crystallogr.* **1978**, *B34*, 268.
- (14) McCrindle, R.; Ferguson, G.; Khan, M. A.; McAalees, A. J.; Ruhl, B. L. *J. Chem. Soc., Dalton. Trans.* **1981**, *4*, 986.
- (15) (a) Chang, T. C. T.; Foxman, B. M.; Rosenblum, M.; Stockman, C. *J. Am. Chem. Soc.* **1981**, *103*, 7361. (b) Watson, L. A.; Franzman, B.; Bollinger, J. C.; Caulton, K. G. *New J. Chem.* **2003**, *27*, 1769. (c) Stoebe, E. J.; Jordan, R. F. *J. Am. Chem. Soc.* **2006**, *128*, 8162. (d) Song, J. S.; Szalda, D. J.; Bullock, R. M. *J. Am. Chem. Soc.* **1996**, *118*, 11134. (e) Cotton, F. A.; Francis, J. N.; Frenz, B. A.; Tsutsui, M. *J. Am. Chem. Soc.* **1973**, *95*, 2483. (f) Sartori, F.; Leoni, L. *Acta Crystallogr.* **1976**, *B32*, 145. (g) Pampaloni, G.; Peloso, R.; Graiff, C.; Tiripicchio, A. *Organometallics* **2005**, *24*, 4475.
- (16) Huang, D.; Bollinger, J. C.; Streib, W. E.; Folting, K.; Young, V.; Eisenstein, O.; Caulton, K. G. *Organometallics* **2000**, *19*, 2281.

- (17) Schenck, H.; Strömberg, S.; Zetterberg, K.; Ludwig, M.; Åkermark, B.; Svensson, M. *Organometallics* **2001**, *20*, 2813.
- (18) Strazisar, S. A.; Wolczanski, P. T. *J. Am. Chem. Soc.* **2001**, *123*, 4728.
- (19) Boyar, E.; Deeming, A. J.; Arce, A. J.; De Sanctis, Y. *J. Organomet. Chem.* **1984**, *276*, C45.
- (20) Luo, S.; Jordan, R. F. *J. Am. Chem. Soc.* **2006**, *128*, 12072.
- (21) Chen, C. L.; Luo, S.; Jordan, R. F. *J. Am. Chem. Soc.* **2008**, *130*, 12892.

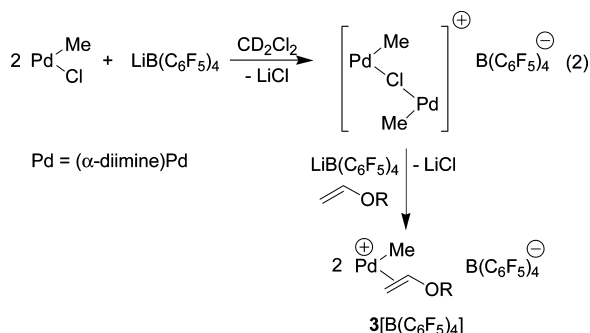
cationic polymerization reactivity of these substrates. We then discuss the reactions of $(\alpha\text{-diimine})\text{PdMe}^+$ with 1 equiv of **2a–g**, under conditions where the concentration of vinyl ether is too low to support cationic polymerization, in order to probe the coordination, insertion, chain-walking, and $\beta\text{-OR}$ elimination reactivity. These studies provide new insights to how to circumvent potential chemical obstacles to the insertion copolymerization of vinyl ethers and olefins.

Results

Generation of $(\alpha\text{-diimine})\text{PdMe}^+$ (1**).** The cationic species $(\alpha\text{-diimine})\text{PdMe}^+$ (**1**) was generated by the methods shown in eq 1 and eq 2. The reaction of $(\alpha\text{-diimine})\text{PdMeCl}$ and $\text{Ag}[\text{SbF}_6]$ in Et_2O generates $[(\alpha\text{-diimine})\text{PdMe}(\text{OEt}_2)][\text{SbF}_6]$ (**1**)[SbF_6], which was isolated as a yellow solid. **1**[SbF_6] is stable in CD_2Cl_2 at -60°C for at least 12 h but decomposes slowly at 20°C .^{2d,22} The Et_2O ligand is readily displaced by vinyl ethers to generate $[(\alpha\text{-diimine})\text{PdMe}(\text{CH}_2=\text{CHOR})][\text{SbF}_6]$ (**3**)[SbF_6] vinyl ether adducts.

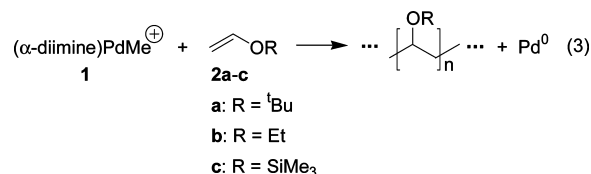


Alternatively, $(\alpha\text{-diimine})\text{PdMe}^+$ was generated in situ by the reaction of $(\alpha\text{-diimine})\text{PdMeCl}$ and $[\text{Li}(\text{Et}_2\text{O})_{2.8}][\text{B}(\text{C}_6\text{F}_5)_4]$ in CD_2Cl_2 at 20°C (eq 2). In the absence of Lewis bases, this reaction produces the dinuclear species $[(\alpha\text{-diimine})\text{PdMe}]_2(\mu\text{-Cl})[\text{B}(\text{C}_6\text{F}_5)_4]$, which is stable at 20°C at least for 24 h, along with an equimolar amount of unreacted $[\text{Li}(\text{Et}_2\text{O})_{2.8}][\text{B}(\text{C}_6\text{F}_5)_4]$.^{4a} In the presence of Lewis bases (L) that are sufficiently strong to displace $(\alpha\text{-diimine})\text{PdMeCl}$ from $[(\alpha\text{-diimine})\text{PdMe}]_2(\mu\text{-Cl})^+$, $(\alpha\text{-diimine})\text{PdMe}(\text{L})^+$ species are formed. This in situ generated cationic system will be referred to as **1**[$\text{B}(\text{C}_6\text{F}_5)_4$] below.



Cationic Polymerization of Vinyl Ethers by **1[$\text{B}(\text{C}_6\text{F}_5)_4$] and **1**[SbF_6].** We first studied the reactions of **1**[$\text{B}(\text{C}_6\text{F}_5)_4$] with excess $\text{CH}_2=\text{CHOR}$ (**2a–g**) to probe trends in cationic polymerization reactivity. As shown in eq 3, the reaction of **1**[$\text{B}(\text{C}_6\text{F}_5)_4$] with excess **2a** at 20°C results in rapid (5 min) and quantitative

polymerization of **2a**. The NMR spectra of the $-\text{[CH}_2\text{CH}(\text{OR})]_n-$ polymer are essentially identical to those of $-\text{[CH}_2\text{CH}(\text{OR})]_n-$ generated by cationic initiators such as $[\text{Ph}_3\text{C}][\text{B}(\text{C}_6\text{F}_5)_4]$ or $[\text{Li}(\text{Et}_2\text{O})_{2.8}][\text{B}(\text{C}_6\text{F}_5)_4]$ under the same conditions. These $-\text{[CH}_2\text{CH}(\text{OR})]_n-$ polymers are atactic ($\text{mm}/\text{mr}/\text{rr} = 1:3:1$) and contain methyl $(-\text{CH}(\text{OR})\text{CH}_3)$, aldehyde $(-\text{CH}_2\text{C}(=\text{O})\text{H})$, and acetal $(-\text{CH}(\text{OR})_2)$ end groups and internal $-\text{CH}=\text{CH}-$ units (ca. 3 mol %).²³ These features are characteristic of a cationic polymerization process.^{10,11,23,24} Interestingly, rapid formation of Pd^0 was observed during the polymerization of **2a**. The reaction of **1**[$\text{B}(\text{C}_6\text{F}_5)_4$] with excess **2b** at 20°C is similar.



The reaction of **1**[$\text{B}(\text{C}_6\text{F}_5)_4$] with a large excess $\text{CH}_2=\text{CHOSiMe}_3$ (**2c**, 50 equiv, 1.2 M) in CD_2Cl_2 at 20°C results in inefficient cationic polymerization to form $-\text{[CH}_2\text{CH}(\text{OSiMe}_3)]_n-$ (7% conversion, 20 h). Pd^0 formation was also observed early in this reaction. However, when less than 10 equiv (0.25 M) of **2c** was used, no cationic polymerization was detected. In contrast, the reaction of **1**[$\text{B}(\text{C}_6\text{F}_5)_4$] with excess **2d–g** (ca. 80 equiv, 2.0 M) in CD_2Cl_2 at 20°C does not generate polymer or Pd^0 .²⁵ The reactions of **1**[SbF_6] with excess **2a–g** gave very similar results.

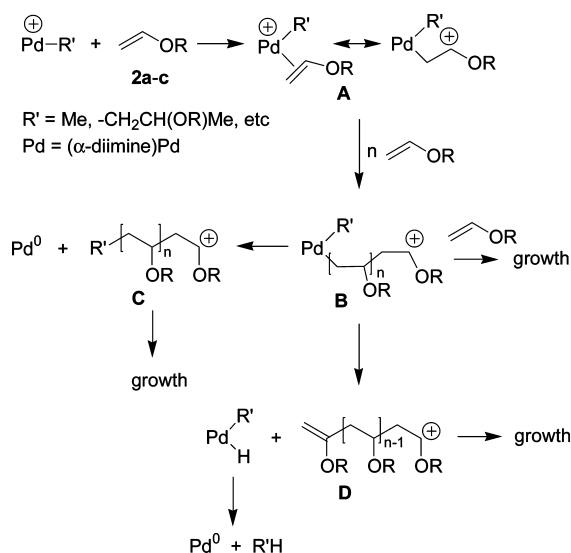
These results imply that the cationic polymerization and Pd^0 formation processes are closely related, and that both processes can be circumvented by using arylsilyl or aryl vinyl ethers.

Initiation of Cationic Polymerization of **2a–c.** Two likely initiators for the cationic polymerization in eq 3 are the $(\alpha\text{-diimine})\text{PdMe}^+$ cation itself or H^+ generated from adventitious water (e.g., via formation of $(\alpha\text{-diimine})\text{PdMe}(\text{H}_2\text{O})^+$). Bulky 2,6-disubstituted pyridines have been used as proton traps to quench the H^+ -initiated cationic polymerization of vinyl ethers and other monomers.^{11f,24b,26} Similarly, pyridine was shown to quench the cationic polymerization of vinyl ethers initiated by $(\text{P}\sim\text{N})\text{PdMe}(\text{H}_2\text{O})^+$ species.^{11b} However, control experiments show that 2,6- $\text{}^t\text{Bu}_2$ -pyridine (DTBP) has only a minimal effect on the rate and yield of the **2a** polymerization in eq 3. This result suggests that $(\alpha\text{-diimine})\text{PdR}^+$ ($\text{R}' = \text{Me}$ or $\text{CH}_2\text{CH}(\text{OR})\text{Me}$ formed by insertion, vide infra) species initiate this reaction.²⁷ A reasonable mechanism for the **1**-mediated polymerization of **2a–c** that accounts for these observations is

- (23) The $-\text{CH}=\text{CH}-$ units are formed by elimination of HOR from the $-\text{[CH}_2\text{CH}(\text{OR})]_n-$ chain. See: Hashimoto, T.; Kanai, T.; Kodaira, T. *J. Polym. Sci., Part A: Polym. Chem.* **1998**, *36*, 675.
- (24) (a) Wang, Q.; Baird, M. C. *Macromolecules* **1995**, *28*, 8021. (b) Kéki, S.; Nagy, M.; Deák, G.; Zsuga, M. *J. Phys. Chem. B* **2001**, *105*, 9896.
- (25) When the in situ generated **1**[$\text{B}(\text{C}_6\text{F}_5)_4$] contains excess $\text{LiB}(\text{C}_6\text{F}_5)_4$, **2d** is slowly cationically polymerized. However, Pd^0 formation was not observed.
- (26) (a) De, P.; Faust, R. *Macromolecules* **2006**, *39*, 7527. (b) Hadjikyriacou, S.; Acar, M.; Faust, R. *Macromolecules* **2004**, *37*, 7543. (c) Bennevault, W.; Peruch, F.; Defieux, A. *Macromol. Chem. Phys.* **1996**, *197*, 2603. (d) Cho, C. G.; Feit, B. A.; Webster, O. W. *Macromolecules* **1992**, *25*, 2081.
- (27) (a) This result may also suggest that $(\alpha\text{-diimine})\text{PdMe}(\text{OH}_2)^+$ is too crowded to be deprotonated by DTBP. It was not possible to test the influence of pyridine on the **1**-initiated cationic polymerization since pyridine displaces the α -diimine ligand. (b) DTBP significantly retards the polymerization of **2a** by $[\text{Li}(\text{Et}_2\text{O})_{2.8}][\text{B}(\text{C}_6\text{F}_5)_4]$.

(22) Johnson, L. K.; Kilian, C. M.; Arthur, S. D.; Feldman, J.; Mccord, E. F.; McLain, S. J.; Kreutzer, K. A.; Bennett, M. A.; Coughlin, E. B. *PCT Int. Appl. WO 9623010*, 1996.

Scheme 3



shown in Scheme 3. Coordination of the vinyl ether to a $(\alpha\text{-diimine})\text{PdR}^+$ species generates an $(\alpha\text{-diimine})\text{-PdR}^+(\text{CH}_2=\text{CHOR})^+$ π complex (**A**), in which the vinyl ether C=C bond is polarized with carbocation character at the substituted carbon (C_{int}), due to the electrophilic character of the cationic Pd center.^{15a,c} Electrophilic attack of C_{int} of **A** on monomer then initiates cationic polymerization. Pd^0 formation can occur by reductive elimination of growing species **B** or more likely by $\beta\text{-H}$ elimination of **B** followed by $\text{R}'\text{-H}$ reductive elimination.^{28,29}

Reaction of $1[\text{SbF}_6]$ or $1[\text{B}(\text{C}_6\text{F}_5)_4]$ with 1 Equiv of $\text{CH}_2=\text{CHOR}$ (2a–g**).** Scheme 3 suggests that it might be possible to probe for vinyl ether insertion chemistry by generating $(\alpha\text{-diimine})\text{PdMe}^+$ species in the presence of stoichiometric quantities of vinyl ether, such that excess substrate is not present to propagate cationic polymerization. Indeed, as shown in the Scheme 4, reaction of **1** $[\text{SbF}_6]$ or **1** $[\text{B}(\text{C}_6\text{F}_5)_4]$ with 1 equiv of **2a–g** proceeds by initial formation of $(\alpha\text{-diimine})\text{PdMe}(\text{CH}_2=\text{CHOR})^+$ (**3a–g**),³⁰ followed by 1,2 insertion to produce $(\alpha\text{-diimine})\text{Pd}(\text{CH}_2\text{CHMeOR})^+$ (**4a–g**) and reversible isomerization to form $(\alpha\text{-diimine})\text{Pd}(\text{CMe}_2\text{OR})^+$ (**5a–g**). The **4a–g**/**5a–g** mixtures react further at 20 °C by $\beta\text{-OR}$ elimination of **4a–g** to generate $(\alpha\text{-diimine})\text{Pd}(\text{OR})(\text{CH}_2=\text{CHMe})^+$ (not observed), followed by allylic C–H activation to yield $(\alpha\text{-diimine})\text{Pd}(\eta^3\text{-C}_3\text{H}_5)^+$ (**6**) and ROH as the ultimate products. These reactions are discussed in detail in the following sections.

Generation of $[(\alpha\text{-Diimine})\text{PdMe}(\text{CH}_2=\text{CHOR})][\text{SbF}_6]$ (3a–g** $[\text{SbF}_6]$).** The reaction of **1** $[\text{SbF}_6]$ and **2a–g** in CD_2Cl_2 at -60 °C generates the corresponding adducts $[(\alpha\text{-diimine})\text{PdMe}(\text{CH}_2=\text{CHOR})][\text{SbF}_6]$ (**3a–g** $[\text{SbF}_6]$) in >90% yield.³¹ No broadening of the ^1H NMR resonances of **3a–g**

Scheme 4

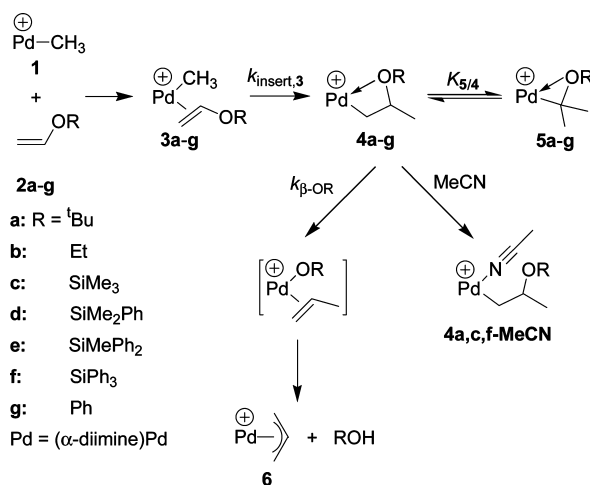


Table 1. ^1H and ^{13}C NMR Chemical Shifts for Free $\text{CH}_2=\text{CHO}^t\text{Bu}$ (**2a**) and **3a** $[\text{SbF}_6]$ (CD_2Cl_2 , -60 °C)

$\text{CH}_2=\text{CHO}^t\text{Bu}$	chemical shift (δ)		Δ^a
resonance	free	coord	
H_{int}	6.47	7.09	−0.62
H_{trans}	4.22	3.27	0.95
H_{cis}	3.93	2.96	0.97
$\text{C}(\text{CH}_3)_3$	1.21	1.35	−0.14
CH_2	90.4	54.4	36.0
CH	147.1	148.2	−1.1
$\text{C}(\text{CH}_3)_3$	76.4	83.6	−7.2

$$^a \Delta = \delta_{\text{free}} - \delta_{\text{coord}}$$

was detected in the presence of excess vinyl ether over the temperature range of -60 to 20 °C, and no EXSY cross peaks between the free and coordinated vinyl ether resonances were observed at -60 or -20 °C. These results show that the exchange between the free and coordinated vinyl ether is slow.

Key NMR data for the *tert*-butyl vinyl ether complex **3a** $[\text{SbF}_6]$ are listed in Table 1. The $\text{CH}_2=\text{CHO}^t\text{Bu}$ ^1H resonance is shifted downfield and the $\text{CH}_2=\text{CHO}^t\text{Bu}$ resonances are shifted upfield from the corresponding resonances of free $\text{CH}_2=\text{CHO}^t\text{Bu}$. Furthermore, the $\text{CH}_2=\text{CHO}^t\text{Bu}$ ^{13}C resonance is shifted significantly upfield, while the OCMe_3 resonance is shifted only slightly upon coordination. These data are characteristic for C=C-bound π complexes, such as $\text{CpFe}(\text{CO})_2\text{-(CH}_2=\text{CHOEt})^+$ and $\text{Cp}'_2\text{Zr}(\text{O}^t\text{Bu})(\eta^2\text{-H}_2\text{C}=\text{CHO}^t\text{Bu})^+$.^{15a,c} In contrast, for O-coordinated $\text{CH}_2=\text{CHOR}$ adducts, such as $(\text{C}_5\text{H}_4\text{Me})_2\text{Zr}(\text{O}^t\text{Bu})(\eta^1\text{-O-EtOCH}=\text{CH}_2)^+$ and $\text{RuH}(\text{CO})(\text{P}^t\text{Bu}_2\text{Me})_2(\eta^1\text{-O-EtOCH}=\text{CH}_2)^+$, the H_{trans} and H_{cis} ^1H NMR resonances are shifted downfield, and the $\text{CH}_2=\text{CHOEt}$ and $\text{CH}_2=\text{CHOCH}_2\text{Me}$ ^{13}C NMR resonances are shifted significantly upfield from those of free vinyl ether.^{15c,16} The NMR spectra of **3b–g** $[\text{SbF}_6]$ are similar to those of **3a** $[\text{SbF}_6]$, showing that these species are also C=C π complexes.

The in situ generated $(\alpha\text{-diimine})\text{PdMe}^+$ system **1** $[\text{B}(\text{C}_6\text{F}_5)_4]$ is less useful for the observation of **3** $[\text{B}(\text{C}_6\text{F}_5)_4]$ complexes because displacement of $(\alpha\text{-diimine})\text{PdMeCl}$ from the intermediate $[(\alpha\text{-diimine})\text{PdMe}]_2(\mu\text{-Cl})^+$ cation (eq 2) by vinyl ethers is slow. **1** $[\text{B}(\text{C}_6\text{F}_5)_4]$ does not react with **2a** in CD_2Cl_2 at -60 °C, indicating that under these conditions the vinyl ether does not break the chloride bridge. However, when the $[(\alpha\text{-diimine})\text{PdMe}]_2(\mu\text{-Cl})^+ / [\text{Li}(\text{Et}_2\text{O})_{2.8}][\text{B}(\text{C}_6\text{F}_5)_4] / \text{2a}$ mixture is warmed to 20 °C for 10 min, $[(\alpha\text{-diimine})\text{PdMe}(\text{CH}_2=\text{CHO}^t\text{Bu})][\text{B}(\text{C}_6\text{F}_5)_4]$ (**3a** $[\text{B}(\text{C}_6\text{F}_5)_4]$) is formed in 78% yield. The

(28) The end groups in species **C** and **D** were not detected by NMR, possibly because their NMR resonances overlap with, and are much weaker than, those of other end groups generated by chain transfer, which is fast (ca. $46\text{-}[\text{CH}_2\text{CH}(\text{O}^t\text{Bu})]_n\text{-chains}$ are produced per Pd). The end group **D** may be incorporated into the polymer.

(29) $(\alpha\text{-Diimine})\text{PdR}_2$ complexes ($\text{R} = \text{Pr}, \text{Bu}, \text{tBu}$) are moderately stable at room temperature. These species slowly decompose (days) to alkanes, alkenes, and unidentified Pd(0) species. See ref 2b.

(30) If the anion is not specified for complexes **3**, **4**, and **5**, the statement is true for both the SbF_6^- and $\text{B}(\text{C}_6\text{F}_5)_4^-$ species. See ref 2b.

(31) The major impurity is $[(\alpha\text{-diimine})\text{PdMe}]_2(\mu\text{-Cl})[\text{SbF}_6]$.

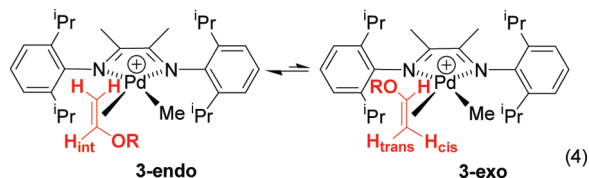
Table 2. Reactivity of CH₂=CHOR with 1[SbF₆]^a

CH ₂ =CHOR (2), R =	Bu (2a)	Et (2b)	SiMe ₃ (2c)	SiMe ₂ Ph (2d)	SiMePh ₂ (2e)	SiPh ₃ (2f)	Ph (2g)
<i>K</i> _{2/ethylene} (−60 °C) ^b	0.88(2)	0.22(1)	0.12(1)				
<i>K</i> _{2/2c} (−20 °C) ^c	5.35 ^d	1.66 ^d	1	0.34(4)	0.19(2)	0.08(1)	0.30(2)
Δ <i>G</i> _{2/2c} (kcal/mol, −20 °C) ^e	−0.8(1)	−0.2(1)	0	0.5(1)	0.8(1)	1.3(1)	0.6(1)
<i>k</i> _{insert,3} (10 ^{−4} s ^{−1} , 0 °C)	0.33(2)	0.84(5)	1.6 (1)	3.2(2)	5.2(3)	8.1(5)	15.0(9)
<i>k</i> _{insert,3} (10 ^{−4} s ^{−1} , 20 °C)	6.3(4)	~27	>33 ^f	>33 ^f	>33 ^f	>33 ^f	>33 ^f
Δ <i>G</i> _{insert,3} (kcal/mol, 0 °C) ^g	21.5(1)	21.0(1)	20.7(1)	20.3(1)	20.0(1)	19.8(1)	19.4(1)
<i>K</i> _{5/4} (0 °C) ^h	0.21	2.2	>19 ⁱ	>19 ⁱ	>19 ⁱ	>19 ⁱ	unknown ^j
<i>K</i> _{5/4} (20 °C) ^h	0.33	2.7	>19 ⁱ	>19 ⁱ	>19 ⁱ	>19 ⁱ	unknown ^j
<i>k</i> _{β-OR,obs} (10 ^{−6} s ^{−1} , 20 °C) ^k	15.0(9)	1200(70)	111(7)	156(9)	246(15)	378(23)	>5000 ^l
<i>k</i> _{β-OR} (10 ^{−6} s ^{−1} , 20 °C) ^m	20(1)	4440(260)	>2220 ⁿ	>3120 ⁿ	>4920 ⁿ	>7560 ⁿ	>5000 ⁿ

^a The uncertainties are based on replicate runs. ^b *K*_{2/ethylene} = [3][CH₂=CH₂][(α-diimine)PdMe(CH₂=CH₂)⁺][−][2][−] at equilibrium. ^c *K*_{2/2c} = [3][2c][3c][−][2][−] at equilibrium. ^d Δ*S* of equilibrium is assumed to be negligible, so Δ*G* does not change over temperature.³³ *K*_{2a,b/ethylene}(−20 °C) = exp{(213/253)ln[*K*_{2a,b/ethylene}(−60 °C)]}; *K*_{2a,b/2c} = *K*_{2a,b/ethylene}/*K*_{2c/ethylene}. ^e Δ*G*_{2/2c} = −*RT*ln*K*_{2/2c}. ^f More than 95% of **3** undergoes insertion within 15 min at 20 °C. ^g The insertion barrier for **3a–g** at 0 °C, Δ*G*_{insert,3} = −*RT*ln(*k*_{insert,3}*h*/*k*_B*T*). ^h *K*_{5/4} = [5]/[4] at equilibrium. ⁱ Complexes **4c–f** were not detected by NMR. ^j **4g** and **5g** were not observed due to fast β-OR elimination of **4g**. ^k The observed first-order rate constant for consumption of the total of **4** and **5**. ^l More than 95% of **3g** is converted to **6** and phenol within 10 min at 20 °C. ^m The first-order rate constant for β-OR elimination of **4**, *k*_{β-OR} = *k*_{β-OR,obs} (*K*_{5/4} + 1). ⁿ Lower limit assuming *K*_{5/4} > 20.

remaining species in solution are [(α-diimine)PdMe]₂(μ-Cl)⁺ (8%) and the insertion products **4a**[B(C₆F₅)₄] (10%) and **5a**[B(C₆F₅)₄] (4%, Scheme 4). Complex **3b**[B(C₆F₅)₄] is formed in 27% yield by the reaction of **1**[B(C₆F₅)₄] and **2b** in CD₂Cl₂ at 20 °C for 10 min. The remaining species in solution are [(α-diimine)PdMe]₂(μ-Cl)⁺ (8%), the insertion products **4b**[B(C₆F₅)₄] (18%) and **5b**[B(C₆F₅)₄] (35%), and allyl complex **6** (12%). Complexes **3c–g**[B(C₆F₅)₄] are not observed in the reaction of **1**[B(C₆F₅)₄] and **2c–g** at 20 °C due to fast insertion.

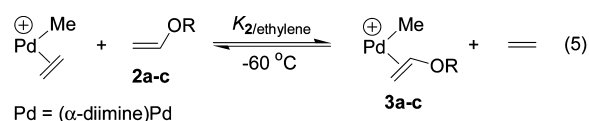
Two rotamers are possible for a (α-diimine)PdMe(CH₂=CHOR)⁺ species, which differ in the orientation of the vinyl ether (eq 4). The ¹H NMR spectra of **3a–g** contain one set of sharp α-diimine, Pd–Me, and vinyl ether resonances over the temperature range of −70 to 20 °C (0 °C for **3g**; insertion is rapid above this temperature), suggesting that either rotation around the Pd–vinyl ether bond is very fast or, more likely, one rotamer is highly favored. NOSEY spectra of **3c–f** contain Pd–Me/CHMe₂, H_{cis}/CHMe₂, and H_{int}/CHMe₂ cross peaks but no cross peaks between the Pd–Me and H_{int} or H_{cis} resonances. These results are consistent with a structure in which the C=C bond is oriented perpendicular to the N–N–Pd–Me square plane and the OR group points toward the Pd–Me group (endo rotamer).³²



To further understand the structures and dynamics of these complexes, two less crowded examples, [(2,6-*i*-Pr₂-C₆H₃)N=CAnCAn=N(2,6-*i*-Pr₂-C₆H₃)]PdMe(CH₂=CHOSiPh₃)[SbF₆] (**3h**, An,An = acenaphthyl) and [(4-Me-C₆H₅)N=CMeCMe=N(4-Me-C₆H₅)]PdMe(CH₂=CHOSiPh₃)[SbF₆] (**3i**) were prepared. **3h** is similar to **3c–f** and exists as the endo isomer. However, at −70 °C in CD₂Cl₂, **3i** exists as a 1/1 mixture of endo and exo rotamers, which were identified by NOSEY correlations. The barrier for olefin rotation (i.e., interconversion of the endo and

exo isomers) of **3i** (Δ*G*_{rotation} = 10.3 kcal/mol, −50 °C) was determined from the coalescence of the Pd–Me resonances.

Competitive Binding of Ethylene and Vinyl Ethers to 1. The relative binding strengths of vinyl ethers **2a–c** to **1**[SbF₆] were determined by competition experiments with ethylene (eq 5). The reactions of **1**[SbF₆] with excess ethylene and **2a–c** were monitored by ¹H NMR at −60 °C until the reaction quotient *Q* = [3][CH₂=CH₂][(α-diimine)PdMe(CH₂=CH₂)⁺][−][2][−] reached a constant value (*K*_{2/ethylene}), indicating that the equilibrium in eq 5 had been reached. **2d–g** bind to Pd much more weakly than ethylene does, so their binding affinities cannot be measured accurately by eq 5. The binding affinities of **2d–g** were determined by competition experiments with **2c** (eq 6). These experiments were conducted at −20 °C in order to accelerate the approach to equilibrium. Equilibrium constants for eq 5 and 6 are listed in Table 2. The reactions of [(α-diimine)PdMe(CH₂=CH₂)]⁺[B(C₆F₅)₄][−] (generated in situ)^{2d} with excess ethylene and **2a–c** gave very similar equilibrium constants (Table 3), showing that the counteranion (SbF₆[−] vs B(C₆F₅)₄[−]) does not strongly influence the relative binding ability of these substrates to **1**.



Pd = (α-diimine)Pd



Pd = (α-diimine)Pd

Insertion of [(α-Diimine)PdMe(CH₂=CHO'Bu)]⁺[B(C₆F₅)₄][−] (3a**[B(C₆F₅)₄]).** The *t*-Bu vinyl ether adduct **3a**[B(C₆F₅)₄] reacts to form [(α-diimine)Pd{CH₂CHMe(O'Bu)}]⁺[B(C₆F₅)₄][−] (**4a**[B(C₆F₅)₄], 66%) and [(α-diimine)Pd{CMe₂(O'Bu)}]⁺[B(C₆F₅)₄][−] (**5a**[B(C₆F₅)₄], 25%) in 2 h at 20 °C (Scheme 4). The first-order rate constant for the consumption of **3a**[B(C₆F₅)₄] was measured by ¹H NMR at 0

(32) (a) Two rotamers of [(2,6-Me₂-C₆H₃)N=CAnCAn=N(2,6-Me₂-C₆H₃)]PdMe(η²-CH₂=CHO₂CCH₃)⁺ were observed. See ref 6. (b) (Me₂bipy)PdMe(η²-CH₂=CHCl)⁺ (Me₂bipy = 4,4'-Me₂-2,2'-bipyridine) prefers the exo structure. See ref 7a.

(33) (a) This assumption was made by Brookhart and by Guan in studies of competitive binding of ethylene and methyl acrylate to (α-diimine)PdR⁺ species. (b) Mecking, S.; Johnson, L. K.; Wang, L.; Brookhart, M. *J. Am. Chem. Soc.* **1998**, *120*, 888. (c) Popeney, C. S.; Guan, Z. B. *J. Am. Chem. Soc.* **2009**, *131*, 12384.

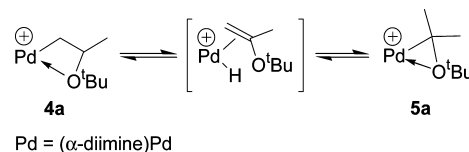
Table 3. Reactivity of CH₂=CHOR with 1[B(C₆F₅)₄]^a

CH ₂ =CHOR (2), R =	^t Bu (2a)	Et (2b)	SiMe ₃ (2c)	SiMe ₂ Ph (2d)	SiMePh ₂ (2e)	SiPh ₃ (2f)	Ph (2g)
<i>K</i> _{2/ethylene} (−60 °C) ^b	1.2(7)	0.21(1)	0.17(1)			<0.01	0.04(1)
<i>k</i> _{insert,3} (10 ^{−4} s ^{−1} , 0 °C)	0.33(2)	0.80(5)					
<i>k</i> _{insert,3} (10 ^{−4} s ^{−1} , 20 °C)	7.1(4)	~20	>33 ^c	>33 ^c	>33 ^c	>33 ^c	>33 ^c
<i>K</i> _{5/4} (0 °C) ^d	0.27	2.5	>19 ^e	>19 ^e	>19 ^e	>19 ^e	>19 ^e
<i>K</i> _{5/4} (20 °C) ^d	0.39	2.8	>19 ^e	>19 ^e	>19 ^e	>19 ^e	unknown ^f
<i>k</i> _{β-OR,obs} (10 ^{−6} s ^{−1} , 20 °C) ^g	2.3(1)	912(55)	32(2)	51(3)	134(8)	107(6)	>5000 ^h
<i>k</i> _{β-OR} (10 ^{−6} s ^{−1} , 20 °C) ⁱ	3.2(2)	3460(200)	>640 ^j	>1020 ^j	>2680 ^j	>2140 ^j	>5000 ^j

^a The uncertainties are based on replicate runs. ^b *K*_{2/ethylene} = [3][CH₂=CH₂][(α-diimine)PdMe(CH₂=CH₂)⁺]^{−1}[2]^{−1} at equilibrium. ^c More than 95% of **3** undergoes insertion within 15 min at 20 °C. ^d *K*_{5/4} = [5]/[4] at equilibrium. ^e Complexes **4c–f** were not detected by NMR. ^f **4g** and **5g** were not observed due to fast β-OR elimination of **4g**. ^g The observed first-order rate constant for consumption of the total of **4** and **5**. ^h More than 95% of **3g** is converted to **6** and phenol within 10 min at 20 °C. ⁱ The first-order rate constant for β-OR elimination of **4**, *k*_{β-OR} = *k*_{β-OR,obs}(*K*_{5/4} + 1). ^j Lower limit assuming *K*_{5/4} > 20.

and 20 °C (Table 3). For the alkyl ligand of **4a**[B(C₆F₅)₄], the ¹H and COSY NMR spectra contain a multiplet at δ 4.86 (CH), a doublet of doublets at δ 0.40 and a triplet at δ 0.93 (CH₂), and a doublet at δ 1.15 (CH₃). For the alkyl ligand of **5a**[B(C₆F₅)₄], the ¹H NMR spectrum comprises a singlet at δ 0.64. NMR data show that both **4a**[B(C₆F₅)₄] and **5a**[B(C₆F₅)₄] contain unsymmetrical α-diimine ligands, indicating that these species are four-coordinate rather than three-coordinate complexes. To probe for O-chelation in **4a** and **5a**, the reaction with CH₃CN was investigated. As shown in Scheme 4, the **4a**[B(C₆F₅)₄]/**5a**[B(C₆F₅)₄] mixture reacts with MeCN in CD₂Cl₂ at −40 °C to produce a single product, (α-diimine)Pd{CH₂CHMe(O^tBu)}(NCMe)⁺ ([**4a**-MeCN][B(C₆F₅)₄]), quantitatively. The PdCH₂CH(O^tBu)Me (δ 67.2) and PdCH₂CH(OCMe₃)Me (δ 72.8) ¹³C NMR resonances of [**4a**-MeCN][B(C₆F₅)₄] appear in the normal range for ^tPr and ^tBu ethers.³⁴ In contrast, the PdCH₂CH(O^tBu)Me (δ 88.3) and PdCH₂CH(OCMe₃)Me (δ 88.9) ¹³C resonances of **4a**[B(C₆F₅)₄] and the PdCMe₂(O^tBu) (δ 82.8) and PdCMe₂(OCMe₃) (δ 90.3) resonances of **5a**[B(C₆F₅)₄] are shifted far downfield from this range, indicating the presence of O-chelation in these species.^{35–38}

Interconversion of **4a[B(C₆F₅)₄] and **5a**[B(C₆F₅)₄].** The **5a**[B(C₆F₅)₄]/**4a**[B(C₆F₅)₄] ratio remains constant (0.39) during the formation of these species from **3a**[B(C₆F₅)₄] at 20 °C and their subsequent conversion to **6** at 20 °C (Scheme 4). These results imply that **4a**[B(C₆F₅)₄] and **5a**[B(C₆F₅)₄] interconvert rapidly on the laboratory time scale but slowly on the NMR chemical shift time scale at this temperature. NMR monitoring studies reveal that, during the reaction of **4a**[B(C₆F₅)₄]/**5a**[B(C₆F₅)₄] with MeCN (1.2 equiv), **4a**[B(C₆F₅)₄] is converted to [**4a**-MeCN][B(C₆F₅)₄] rapidly (within 5 min at −60 °C), while **5a**[B(C₆F₅)₄] is converted to [**4a**-MeCN][B(C₆F₅)₄] slowly (ca.

Scheme 5

140 min at −40 °C). The adduct [**5a**-MeCN][B(C₆F₅)₄] was not detected. Therefore, at this temperature, **5a**[B(C₆F₅)₄] slowly rearranges to **4a**[B(C₆F₅)₄], which is then rapidly trapped by MeCN (Scheme 4).

The interconversion of **4a**[B(C₆F₅)₄] and **5a**[B(C₆F₅)₄] occurs by a normal chain-walking mechanism, that is, β-H elimination to generate (α-diimine)PdH(CH₂=CMe(O^tBu))⁺ (not observed) followed by re-insertion (Scheme 5). DFT studies show that the energy difference between **4a**[B(C₆F₅)₄] and **5a**[B(C₆F₅)₄] is small (*E*_{4a} − *E*_{5a} = 0.2 ± 1.0 kcal/mol), which is consistent with the fact that both isomers are observed.

Conversion of **4a[B(C₆F₅)₄] and **5a**[B(C₆F₅)₄] to (α-diimine)Pd(η³-C₃H₅)[B(C₆F₅)₄] (**6**[B(C₆F₅)₄]).** The **4a**[B(C₆F₅)₄]/**5a**[B(C₆F₅)₄] mixture reacts to produce (α-diimine)Pd(η³-C₃H₅)[B(C₆F₅)₄] (**6**[B(C₆F₅)₄]) and ^tBuOH quantitatively over the course of 15 days at 20 °C in CD₂Cl₂ solution (Scheme 4). Compound **6**[B(C₆F₅)₄] was prepared independently and fully characterized.

The most likely mechanism for the conversion of **4a**[B(C₆F₅)₄]/**5a**[B(C₆F₅)₄] to **6**[B(C₆F₅)₄] is β-OR elimination of **4a**[B(C₆F₅)₄] to generate (α-diimine)Pd(OR)(CH₂=CHMe)⁺ (not observed), followed by allylic C–H activation (Scheme 4). Similar C–H activation reactions to form allyl species were reported by Bercaw for α-diimine Pt and Pd hydroxide complexes.³⁹ In related work, Hosokawa showed that in situ generated CIP-d(OH)(propene) undergoes allylic C–H activation to form {(π-allyl)PdCl}₂ and H₂O.⁴⁰ Also, the reaction of Pd(II) chloride salts with α-olefins to generate (π-allyl)Pd(II) complexes is well-known.⁴¹

As noted above, the **5a**[B(C₆F₅)₄]/**4a**[B(C₆F₅)₄] ratio remains constant during the conversion of **4a**[B(C₆F₅)₄]/**5a**[B(C₆F₅)₄] to **6**[B(C₆F₅)₄], indicating that the **4a**[B(C₆F₅)₄]/**5a**[B(C₆F₅)₄] exchange is faster than the β-O^tBu elimination of **4a**[B(C₆F₅)₄].

(34) ¹³C NMR (CDCl₃): Me₂CHOCMe₃, δ 63.4; Me₂CHO CMe₃, δ 72.7.

(35) The possible coordination of the excess CH₂=CHO^tBu or Et₂O present in solution was ruled out because NMR data show that these species are free. After removal of volatiles from the mixture, the NMR resonances for **4a** and **5a** are unchanged, confirming that excess CH₂=CHO^tBu and Et₂O do not bind to these species. β-H agostic interactions were not detected in **4a**[B(C₆F₅)₄] and **5a**[B(C₆F₅)₄] by ultra-low-temperature NMR (CDCl₂F solution, −130 °C). Under similar conditions (CDCl₂F, −120 °C), the ¹H NMR resonance for the agostic H in (α-diimine)Pd{CH(CH₂-μ-*H*)CH₃}⁺ (δ = −7.85) was observed. See ref 2d.

(36) For comparison, the O(CH₂CH₃)₂ ¹³C NMR resonance for (α-diimine)PdMe(OEt)₂⁺ appears at δ 71.5, while the corresponding resonance for free O(CH₂CH₃)₂ appears at δ 65.7. See ref 2e.

(37) O-Chelation in the analogous species Ru(η²-CH₂CH₂OCH₃)(CO)(P^tBu₂Me)₂⁺ was established by X-ray diffraction. The RuCH₂CH₂OCH₃ and RuCH₂CH₂OCH₃ ¹³C NMR resonances occur at δ 89.6 and 60.6 ppm, respectively. See ref 16.

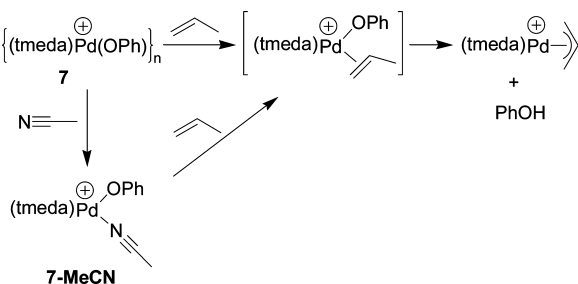
(38) DFT calculations confirmed that **4** and **5** have O-chelated structures. See the Supporting Information.

(39) (a) Driver, T. G.; Williams, T. J.; Labinger, J. A.; Bercaw, J. E. *Organometallics* **2007**, 26, 294. (b) Bercaw, J. E.; Hazari, N.; Labinger, J. A.; Oblad, P. F. *Angew. Chem., Int. Ed.* **2008**, 47, 9941. (c) Williams, T. J.; Caffyn, A. J. M.; Hazari, N.; Oblad, P. F.; Labinger, J. A.; Bercaw, J. E. *J. Am. Chem. Soc.* **2008**, 130, 2418.

(40) Hosokawa, T.; Tsuji, T.; Mizumoto, Y.; Murahashi, S. I. *J. Organomet. Chem.* **1999**, 574, 99.

(41) (a) Morellir, D.; Ugo, R.; Conti, F.; Donati, M. *Chem. Commun.* **1967**, 16, 801. (b) Ketley, A. D.; Braatz, J. *Chem. Commun.* **1968**, 3, 169.

Scheme 6



Therefore, the conversion of **4a**[B(C₆F₅)₄]/**5a**[B(C₆F₅)₄] to **6**[B(C₆F₅)₄] obeys pre-equilibrium kinetics. The observed first-order rate constant $k_{\beta\text{-O}^t\text{Bu,obs}}$ for consumption of the total of **4a**[B(C₆F₅)₄] and **5a**[B(C₆F₅)₄] and the formation of **6**[B(C₆F₅)₄] was measured by ¹H NMR. The first-order rate constant for $\beta\text{-O}^t\text{Bu}$ elimination ($k_{\beta\text{-O}^t\text{Bu}}$) of **4a**[B(C₆F₅)₄] is given by eq 7.⁴² Values for these rate constants are listed in Table 3.

$$k_{\beta\text{-O}^t\text{Bu}} = k_{\beta\text{-O}^t\text{Bu,obs}}(K_{5a/4a} + 1) \quad (7)$$

Model Allylic C–H Activation Reaction. Attempts to prepare discrete (α -diimine)Pd(OR)⁺ species to probe if they react with propene by allylic C–H activation as proposed in Scheme 4 were unsuccessful. However, the model compound [(tmeda)Pd(OPh)]_n[B(C₆F₅)₄]_n (**7**, tmeda = *N,N,N',N'*-tetramethyl ethylenediamine) was generated in situ by the reaction of (tmeda)Pd(OPh)₂⁴³ with [HNMe₂Ph][B(C₆F₅)₄]. The base-free species **7** is believed to be a labile oligomer in solution (see Experimental Section). Complex **7** reacts with MeCN to generate the monomeric species [(tmeda)Pd(OPh)(NCMe)][B(C₆F₅)₄] (**7-MeCN**). Both **7** and **7-MeCN** react with propylene to produce [(tmeda)Pd($\eta^3\text{-C}_3\text{H}_5$)] [B(C₆F₅)₄] and phenol at 20 °C (Scheme 6). The propylene complex [(tmeda)Pd(OPh)(CH₂=CHMe)] [B(C₆F₅)₄] was not detected by NMR monitoring of these reactions, which suggests that the allylic C–H activation step is facile.

Reaction of 1[SbF₆] with 2a. The reaction of 1[SbF₆] with **2a** is similar to that of 1[B(C₆F₅)₄] with **2a**, and the NMR data for **5a**[SbF₆]/**4a**[SbF₆] are very similar to those for **5a**[B(C₆F₅)₄]/**4a**[B(C₆F₅)₄]. The insertion rate constant ($k_{\text{insert},3a}$) and equilibrium constant ($K_{5a/4a}$) are also very similar for both cases (Table 2). However, the $\beta\text{-OR}$ elimination rate constant of **4a**[SbF₆] ($k_{\beta\text{-OR}}$) is 6.5 times greater than that of **4a**[B(C₆F₅)₄] (Tables 2 and 3).

Reactions of 1[B(C₆F₅)₄] and 1[SbF₆] with 2b–g. The key features of these reactions that are different from the reactions of **2a** are summarized in this section, and key equilibrium and rate constants are given in Tables 2 and 3. Ethyl vinyl ether (**2b**) binds less strongly than 1[B(C₆F₅)₄] but inserts more rapidly compared to **2a**. Interestingly, while $K_{5b/4b}$ is greater than $K_{5a/4a}$, $\beta\text{-OEt}$ elimination of **4b** is 10³ faster than $\beta\text{-O}^t\text{Bu}$ elimination of **4a**. Similar results are observed for the reaction of 1[SbF₆] with **2b**. The insertion rate constant ($k_{\text{insert},3b}$) and equilibrium constant ($K_{5b/4b}$) are very similar for both the [B(C₆F₅)₄][−] and [SbF₆][−] anions, while the $\beta\text{-OR}$ elimination rate constant of **4b**[SbF₆] ($k_{\beta\text{-OR}}$) is 1.3 times greater than that of **4b**[B(C₆F₅)₄].

The reactions of 1[SbF₆] with **2c–g** are similar to those with **2a**. The insertion rate constant $k_{\text{insert},3}$ of the silyl vinyl ether

complexes at 0 °C follows the order **3f** > **3e** > **3d** > **3c**. However, the formation of **3c–f**[B(C₆F₅)₄] from the reaction of 1[B(C₆F₅)₄] with **2c–f** is slower than the subsequent insertion reactions, so accurate $k_{\text{insert},3}$ values could not be obtained in these cases.

The direct insertion products **4c–f** were not detected by NMR, which implies that $K_{5c-f/4c-f}$ > 19. DFT studies show that both **4c** and **5c** have O-chelated structures and that **5c** is 3.6 ± 1 kcal/mol more stable than **4c**, consistent with the fact that only **5c** is observed. **5c,f**[B(C₆F₅)₄] react with MeCN to afford [4c,f-MeCN][B(C₆F₅)₄] in >90% yield, which confirms that **4c,f**[B(C₆F₅)₄] and **5c,f**[B(C₆F₅)₄] readily interconvert.

Complexes **5c–f** react to generate **6** (100%) and ROH via rearrangement to **4c–f** followed by $\beta\text{-OR}$ elimination and allylic C–H activation. In the case of **5c,d**, the ROH products react further to yield R₂O and H₂O. The observed $\beta\text{-OR}$ elimination rate constant ($k_{\beta\text{-OR,obs}}$) follows the order **f** > **e** > **d** > **c**. As observed for **2a,b**, the observed $\beta\text{-OR}$ elimination rate constant of **4c–f**/**5c–f**[SbF₆] ($k_{\beta\text{-OR,obs}}$) is greater than that of **4c–f**/**5c–f**[B(C₆F₅)₄].

NMR monitoring studies of the reaction of phenyl vinyl ether complex **3g** (B(C₆F₅)₄[−] and SbF₆[−] salts) at 0–20 °C reveal smooth quantitative conversion to **6** and phenol. Neither the 1,2 insertion product **4g** nor its chain-walk isomer **5g** was detected, which indicates that $\beta\text{-OPh}$ elimination of **4g** is fast.⁴⁴

Other α -Diimine Ligands. The insertion rate constant of sterically open **3h** ($k_{\text{insert}} = 2.0 \times 10^{-4} \text{ s}^{-1}$ at 0 °C) is 4 times smaller than that of **3f** ($8.1 \times 10^{-4} \text{ s}^{-1}$ at 0 °C). This difference is consistent with the trend observed in analogous ethylene insertion reactions.^{2d,45} The $\beta\text{-OSiPh}_3$ elimination rate of [(2,6-*i*-Pr₂-C₆H₃)N=CAnCAn=N(2,6-*i*-Pr₂-C₆H₃)]PdCMe₂(OSiPh₃)]-[SbF₆] (**5h**) ($k_{\beta\text{-OSiPh}_3, \text{obs}} = 1.37 \times 10^{-4} \text{ s}^{-1}$ at 20 °C) is also slower than that of **5f** ($k_{\beta\text{-OSiPh}_3, \text{obs}} = 3.78 \times 10^{-4} \text{ s}^{-1}$ at 20 °C). These results show that decreasing the steric crowding around the Pd center decreases the rate of both the CH₂=CHOSiPh₃ insertion and $\beta\text{-OSiPh}_3$ elimination reactions.

Discussion

The results described above provide insights into the cationic polymerization and insertion processes observed in the reactions of vinyl ethers with (α -diimine)PdMe⁺ (**1**). First, the efficiency of **1**-initiated cationic polymerization varies in the order CH₂=CHO^{*t*}Bu (**2a**) > CH₂=CHOEt (**2b**) > CH₂=CHOSiMe₃ (**2c**), and this process is not observed for CH₂=CHOSiMe₂Ph (**2d**), CH₂=CHOSiMePh₂ (**2e**), CH₂=CHOSiPh₃ (**2f**), or CH₂=CHOPh (**2g**). The **1**-initiated cationic polymerization of **2a,b** and the corresponding Pd⁰ formation preclude the use of these vinyl ethers as comonomers in olefin polymerization (Scheme 1).²⁰ The **1**-initiated cationic polymerization of **2c** is fast enough to compete with **1**-initiated 1-hexene/**2c** insertion copolymerization and renders this process inefficient.

The trend in the efficiency of **1**-initiated cationic polymerization rate, **2a** > **2b** > **2g**, is consistent with the classical trend for cationic polymerization by other initiators.^{10–12,46} The key

(42) Wright, M. R. *An Introduction to Chemical Kinetics*; John Wiley & Sons: New York, 2004; p 346.

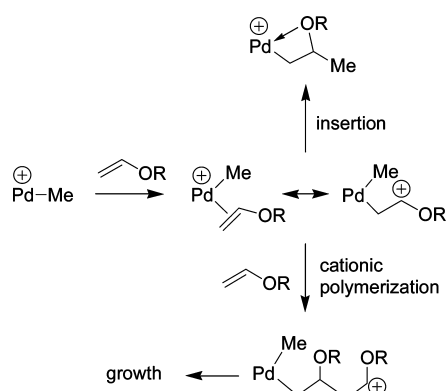
(43) Alsters, P. L.; Baesjou, P. J.; Janssen, M. D.; Kooijman, H.; Roetman, A. S.; Spek, A. L.; Koten, G. V. *Organometallics* **1992**, *11*, 4124.

(44) 2,6-Dimethylphenyl vinyl ether, 2-*tert*-butylphenyl vinyl ether, pentafluorophenyl vinyl ether, and 4-nitrophenyl vinyl ether react similarly to **2g**.

(45) Consistent with this trend, the insertion of **3i** ($k_{\text{insert},3i} = 1.76 \times 10^{-4} \text{ s}^{-1}$ at 0 °C) is slower than that of **3f** or **3h**. However, in this case, the insertion product is not stable and multiple species and Pd⁰ are formed.

(46) (a) Aoki, S.; Stille, J. K. *Macromolecules* **1970**, *3*, 473. (b) Plesch, P. H.; Shamliam, S. H. *Eur. Polym. J.* **1990**, *26*, 1113. (c) Shildknecht, C. E.; Zoss, A. O.; Grosser, F. *Ind. Eng. Chem.* **1949**, *41*, 2891. (d) Matsumoto, H. J.; Okamura, S. *Kobunshi Kagaku* **1968**, *26*, 702.

Scheme 7



parameter that influences the reactivity of these substrates is the electron-donating ability of the OR group, which activates the C=C bond for electrophilic attack and stabilizes the growing alkoxy carbenium ion.⁴⁷ It is surprising that **2c–f** are not cationically polymerized by **1** since silyl vinyl ethers including **2c,d** are readily polymerized by Lewis acids such as EtAlCl₂, SnCl₄, TiCl₄, and BF₃.⁴⁸ Moreover, kinetic studies of the reactions of Ar₂CH⁺ cations with vinyl ethers show that silyl vinyl ethers have similar or higher nucleophilicity compared to analogous alkyl vinyl ethers.⁴⁹ Also, we showed that Ag[SbF₆], [Li(OEt)₂][B(C₆F₅)₄], [Ph₃C][B(C₆F₅)₄], and [H(OEt)₂][B(C₆F₅)₄] initiate cationic polymerization of **2c–g** under the conditions studied here. The low efficiency (**2c**) or absence (**2d–f**) of cationic polymerization of **2c–f** by **1** is due to competing insertion chemistry, which consumes **1**. As noted above, **1**[B(C₆F₅)₄] undergoes up to three sequential insertions of **2f**, ultimately forming Pd allyl products (Scheme 2).²¹ Analogous multiple insertion reactions occur for **2c–f**. Similarly, it is surprising that **2g** is not cationically polymerized by **1** since other cationic initiators such as [4-ClC₆H₄CO][SbF₆] and SnCl₄ readily polymerize this monomer.⁵⁰ In this case, fast insertion and β-Oph elimination out-compete cationic polymerization and produce (α-diimine)Pd(η³-C₃H₅) (**6**) and PhOH (Scheme 1). The Pd allyl products of these reactions are not active for cationic polymerization.

The competition between cationic polymerization, which dominates for **2a,b**, and insertion chemistry, which dominates for **2d–g**, is controlled by the relative rates of these processes (Scheme 7). As noted above, literature data suggest that the inherent reactivity of alkyl and silyl vinyl ethers toward cationic polymerization is similar, which in turn suggests that the key factor that influences the competition between polymerization and insertion is the insertion rate constant of the (α-

diimine)PdMe(CH₂=CHOR)⁺ adduct (*k*_{insert,3}). The *k*_{insert,3a,b} values are relatively small, so cationic polymerization dominates for **2a,b**. However, the *k*_{insert,3d–g} values are more than 4 times larger than *k*_{insert,3b}, and thus insertion chemistry predominates for **2d–g**. The value for *k*_{insert,3c} is only 2 times larger than *k*_{insert,3b}, and both insertion and cationic polymerization proceed for **2c**; the latter process is favored at higher **2c** concentrations because it is first-order in **2c**, while the insertion of **3c** is zero-order in **2c**.

It should be noted that, in some cases, cationic polymerization of silyl vinyl ethers is terminated or prevented by desilylation of the growing siloxy carbenium ion by nucleophilic attack at the SiR₃ group to yield oligomers or polymers with –CH₂C(=O)R end groups. For example, Rimmer showed that the reaction of CH₂=CHO'Bu and CH₂=CPh(OSiMe₃) with a HCl·CH₂=CHO'Bu/TiCl₄ initiator system yields oligomers of general structure H(CH₂CHO'Bu)_nCH₂C(=O)Ph.⁵¹ This reaction proceeds by cationic polymerization of CH₂=CHO'Bu, occasional addition of the growing alkoxy carbenium ion to CH₂=CPh(OSiMe₃) to yield H(CH₂CHO'Bu)_nCH₂CPh(OSiMe₃)⁺, and reaction with Cl[–] to yield H(CH₂CHO'Bu)_nCH₂C(=O)Ph and Me₃SiCl. Desilylations of this type can occur when Cl[–] or F[–] are present.⁵² Several lines of evidence establish that the absence of cationic polymerization of **2d–f** by **1** is not due to such desilylation reactions. First, essentially quantitative yields of the Pd allyl products derived from multiple insertion, but no aldehyde products, are observed in the reaction of **1** with excess CH₂=CHSiPh₃ (**2f**, Scheme 2). Second, the relatively stable, poorly nucleophilic anions [SbF₆][–] or [B(C₆F₅)₄][–] are used as counterions for **1**. Third, as noted above, Ag[SbF₆], [Li(OEt)₂][B(C₆F₅)₄], [Ph₃C][B(C₆F₅)₄], and [H(OEt)₂][B(C₆F₅)₄] all initiate cationic polymerization of **2c–f** under the conditions studied here.⁵³

Liu et al. reported that [(1-PPh₂-2-N=CHAr–C₆H₄)–PdMe(H₂O)][BF₄] (Ar = 4-FC₆H₄, C₆H₅) initiates fast cationic polymerization of alkyl vinyl ethers but not of CH₂=CHOSiMe₃.^{11c} Our results suggest that insertion chemistry similar to that observed for (α-diimine)PdMe⁺ may out-compete cationic polymerization in the latter case.

Under conditions where the cationic polymerization is circumvented, that is, by using low concentrations of **2a–c** or by using **2d–g**, the vinyl ether undergoes the C=C π coordination, insertion, chain-walking, β-OR elimination, and allylic C–H activation process shown in Scheme 4. The relative binding strengths of CH₂=CHOR vary in the order CH₂=CHO'Bu (**2a**) > CH₂=CHOEt (**2b**) ~ CH₂=CHOSiMe₃ (**2c**) > CH₂=CHOSiMe₂Ph (**2d**) ~ CH₂=CHOPh (**2g**) > CH₂=CHOSiMePh₂ (**2e**) > CH₂=CHOSiPh₃ (**2f**). The binding strength trend reflects a combination of electronic and steric effects. The σ-donation component dominates the Pd–olefin bonding in (α-diimine)PdR(olefin)⁺ species due to the poor

- (47) (a) Yuki, H.; Hatada, K.; Nagata, K.; Emura, T. *Polym. J.* **1970**, *1*, 269. (b) Hatada, K.; Nagata, K.; Yuki, H. *Bull. Chem. Soc. Jpn.* **1970**, *43*, 3195. (c) Hatada, K.; Nagata, K.; Hasegawa, T.; Yuki, H. *Makromol. Chem.* **1977**, *178*, 2413. (d) Hatada, K.; Kitayama, T.; Nishiura, T.; Shibuya, W. *J. Polym. Sci., Part A* **2002**, *40*, 2134.
- (48) (a) Murahashi, S.; Nozakura, S.; Sumi, M. *J. Polym. Sci., Part B* **1965**, *3*, 245. (b) Nozakura, S.; Ishihara, S.; Inaba, Y.; Matsumura, K.; Murahashi, S. *J. Polym. Sci.* **1973**, *11*, 1053. (c) Solaro, R.; Chiellini, E. *Gazz. Chim. Ital.* **1976**, *106*, 1037. (d) Palos, I.; Cadenas-Pliego, G.; Knjazhanski, S. Y.; Jimenez-Regalado, E. J.; Casas, E. G. D.; Ponce-Ibarra, V. H. *Polym. Degrad. Stab.* **2005**, *90*, 264.
- (49) (a) Bartl, J.; Steenken, S.; Mayr, H. *J. Am. Chem. Soc.* **1991**, *113*, 7710. (b) Burfeindt, J.; Patz, M.; Muller, M.; Mayr, H. *J. Am. Chem. Soc.* **1998**, *120*, 3629.
- (50) (a) Plesch, P. H.; Shamlian, S. H. *Eur. Polym. J.* **1990**, *26*, 1113. (b) Heublein, G.; Wondraczek, R. *Acta Polym.* **1980**, *31*, 558. (c) Yamamoto, K.; Higashimura, T. *Polymer* **1975**, *16*, 815.

- (51) (a) Lang, W. H.; Sarker, P. K.; Rimmer, S. *Macromol. Chem. Phys.* **2004**, *205*, 1011. (b) Sarker, P. K.; Rimmer, S. *Macromol. Chem. Phys.* **2005**, *206*, 1280.
- (52) (a) Sawamoto, M.; Okamoto, C.; Higashimura, T. *Macromolecules* **1987**, *20*, 2693. (b) Cramail, H.; Deffieux, A. *J. Phys. Org. Chem.* **1995**, *8*, 293. (c) Kuwajima, I.; Nakamura, E.; Shimizu, M. *J. Am. Chem. Soc.* **1982**, *104*, 1025. (d) Huffman, J. W.; Potnis, S. M.; Satish, A. V. *J. Org. Chem.* **1985**, *50*, 4266.
- (53) It is highly unlikely that the LiCl that is generated as a byproduct in situ activation of (α-diimine)PdMeCl with [Li(OEt)₂][B(C₆F₅)₄] inhibits or prevents cationic polymerization of **2c–g** because LiCl is not soluble in CD₂Cl₂, and the discrete catalyst **1**[SbF₆] does not initiate cationic polymerization of **2c–g**.

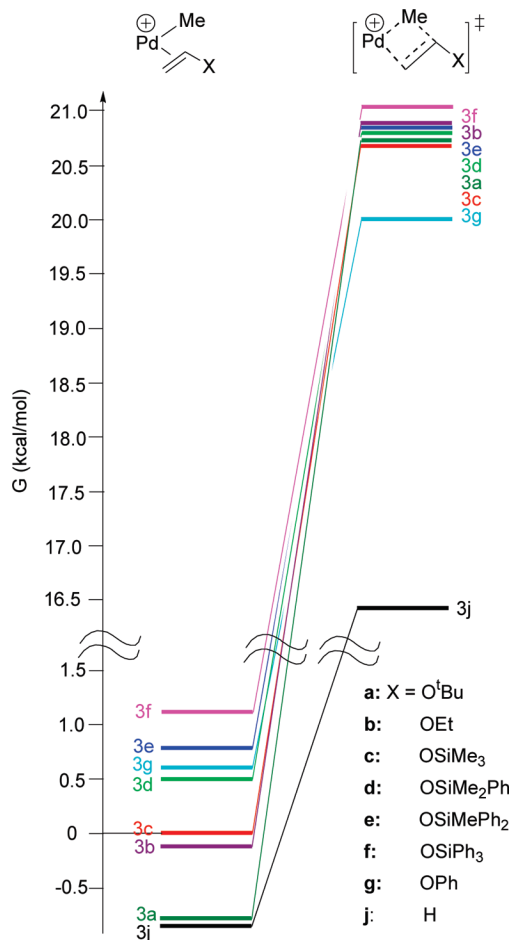


Figure 1. Energy diagram for insertion of **3a–g**[SbF₆]. Relative ground-state energies (versus **3c**) are based on $K_{2/\text{ethylene}}$ and $K_{2/\text{2c}}$ values in Table 2. Transition-state energies are based on $k_{\text{insert},3}$ data in Table 2. ΔG^\ddagger for **3j** is based on the $k_{\text{insert,ethylene}}$ value in ref 2d.

back-bonding ability of the cationic Pd(II) center.⁵⁴ The trend in binding strengths, **2a** > **2c** > **2g**, parallels the trend in the DFT-calculated HOMO energies **2a** (−5.76 eV) > **2c** (−5.86 eV) > **2g** (−5.95 eV).^{17,55} The DFT-calculated HOMO energies of **2c** and **2b** (−5.89 eV) are similar, but **2c** is more sterically bulky and hence binds more weakly compared to **2b**. The trend in binding strength **2c** > **2d** > **2e** > **2f** is expected because these substrates become poorer donors and more sterically crowded as methyl groups are replaced by phenyl groups.

The vinyl ether adducts **3a–g**[SbF₆] undergo insertion with exclusively 1,2 regioselectivity. The insertion rate constants ($k_{\text{insert},3}$, Table 2) vary in the order **3a** < **3b** < **3c** < **3d** < **3e** < **3f** < **3g**. An energy diagram for the insertion of **3a–g** and (α -diimine)PdMe(ethylene)⁺ based on ground-state energies (versus **3c**) derived from competitive binding studies ($K_{2/\text{ethylene}}$ and $K_{2/\text{2c}}$ in Table 2) and insertion barriers determined from insertion rate constants ($k_{\text{insert},3}$, Table 2; $k_{\text{insert,ethylene}} = 900 \times 10^{-4} \text{ s}^{-1}$ at 0 °C^{2d}) is shown in Figure 1. The major factor contributing to

the difference in the insertion barriers of **3a–g** is the ground-state energy of the vinyl ether adduct. As noted above, strongly electron-donating OR groups increase the binding strength and hence lower the ground-state energy and increase the insertion barrier, while steric crowding has the opposite effect.^{2d} Complexes **3a–g** all insert more slowly than (α -diimine)PdMe(ethylene)⁺.

The 1,2 insertion products (α -diimine)Pd{CH₂CH(OR)Me}⁺ (**4a–f**) rapidly and reversibly isomerize to the chain-walk isomers (α -diimine)Pd{CMe₂(OR)}⁺ (**5a–f**) via β -H elimination/reinsertion. The equilibrium constants $K_{5/4}$ increase in the order $K_{5a/4a} < K_{5b/4b} \ll K_{5c-f/4c-f}$ (only **5** is observed), showing that as the R group changes from alkyl to silyl the preference for **5** versus **4** increases. This trend may reflect the trend in electron-donating ability of the OR group O^tBu > OEt > OSiR₃.⁵⁶ Previous studies have shown that L_nM–R bonds are strengthened by the presence of electron-withdrawing substituents on C _{α} of the R group, which can stabilize the δ^- charge on C _{α} resulting from the inherent polarization of the M–C bond.⁵⁷ Electron-donating groups are expected to exert the opposite effect, so strongly electron-donating –OR groups exhibit small $K_{5/4}$ values. Steric factors may also influence $K_{5/4}$; however, this issue is difficult to assess since the relative steric crowding in **4** versus **5** will be sensitive to the identity of the OR group.

Complexes **4a–g** undergo β -OR elimination. The observed β -OR elimination rate constants for the **4/5** mixtures ($k_{\beta\text{-OR,obs}}$) vary in the order O^tBu < OSiR₃ < OPh. This trend parallels the expected order of leaving group ability [−]O^tBu < [−]OSiR₃ < [−]OPh.⁵⁸ β -OR elimination is also more facile for small OR groups; for example, β -OEt elimination is much faster than β -O^tBu elimination.⁵⁹ The fast β -OAr elimination of **4g** and analogous (α -diimine)PdCH₂CHOAr⁺ species⁴⁴ precludes the use of aryl vinyl ethers as comonomers in 1-catalyzed olefin polymerization (Scheme 1).

The data in Tables 2 and 3 show that the anion (SbF₆[−] vs B(C₆F₅)₄[−]) has only a small influence on the vinyl ether binding strength ($K_{2a-c/\text{ethylene}}$), the vinyl ether insertion rates ($k_{\text{insert},3}$), or subsequent chain-walking ($K_{5/4}$). However, the $k_{\beta\text{-OR,obs}}$ values for **4a–f**[SbF₆]/**5a–f**[SbF₆] are 1.3 to 6.5 times greater than

(54) (a) Burns, C. T.; Jordan, R. F. *Organometallics* **2007**, *26*, 6726. (b) Burns, C. T.; Jordan, R. F. *Organometallics* **2007**, *26*, 6737. (c) Willner, H.; Aubke, F. *Organometallics* **2003**, *22*, 3612. (d) Lupinetti, A. J.; Strauss, S. H.; Frenking, G. *Prog. Inorg. Chem.* **2001**, *49*, 1. (e) Rix, F. C.; Brookhart, M. *J. Am. Chem. Soc.* **1995**, *117*, 1137. (f) Rix, F. C.; Brookhart, M.; White, P. S. *J. Am. Chem. Soc.* **1996**, *118*, 4746. (55) (a) Kačer, P.; Tobičik, J.; Kuzma, M.; Červený, L. *J. Mol. Catal. A* **2003**, *195*, 235.

(56) The electron-donating ability trend O^tBu > OEt > OSiR₃ parallels the order of pK_a values of the conjugate acids HOR: HO^tBu (17) > HOEt (15.9) > HO^tSiMe₃ (12.7) > HO^tSiPh₃ (10.8). (57) (a) Axe, F. U.; Marynick, D. S. *J. Am. Chem. Soc.* **1988**, *110*, 3728. (b) Cotton, J. D.; Markwell, R. D. *J. Organomet. Chem.* **1990**, *388*, 123. (c) Cotton, J. D.; Crisp, G. T.; Daly, V. A. *Inorg. Chim. Acta* **1981**, *47*, 165. (d) Cross, R. J.; Gemmill, J. J. *Chem. Soc., Dalton Trans.* **1981**, 2317. (e) Cawse, J. N.; Fiato, R. A.; Pruett, R. L. *J. Organomet. Chem.* **1979**, *172*, 405. (f) Anderson, G. K.; Cross, R. J. *Acc. Chem. Res.* **1984**, *17*, 67. (g) Kuhlmann, E. J.; Alexander, J. J. *Coord. Chem. Rev.* **1980**, *33*, 195. (h) Calderazzo, F.; Noack, K. *Coord. Chem. Rev.* **1966**, *1*, 118. (i) Koga, N.; Morokuma, K. *J. Am. Chem. Soc.* **1986**, *108*, 6136. (j) Galamb, V.; Pályi, G.; Boese, R.; Schmid, G. *Organometallics* **1987**, *6*, 861. (k) Clot, E.; Besora, M.; Maseras, F.; Mégret, C.; Eisenstein, O.; Oelckers, B.; Perutz, R. N. *Chem. Commun.* **2003**, 490. (l) Clot, E.; Mégret, C.; Eisenstein, O.; Perutz, R. N. *J. Am. Chem. Soc.* **2009**, *131*, 7817. (m) Evans, M. E.; Burke, C. L.; Yaibuathes, S.; Clot, E.; Eisenstein, O.; Jones, W. D. *J. Am. Chem. Soc.* **2009**, *131*, 13464. (58) As noted by Caulton, since β -OR elimination implies migration of the RO[−] anion, OPh should be more prone to migrate than OEt. (a) Ozerov, O. V.; Watson, L. A.; Pink, M.; Caulton, K. G. *J. Am. Chem. Soc.* **2004**, *126*, 6363. (b) The order of leaving ability of OR groups is inverse to the order of pK_a values of their conjugate acids HO R: HO^tBu > HOEt > HO^tSiR₃ > HO^tPh (9.8). (59) (a) The fact that [−]O Et is a better leaving group than [−]O^tBu also contributes. (b) The β -OR elimination of (tBu₃SiO)₃TaH(CH₂CH₂OR) is much slower for R = ^tBu than R = Et. See ref 18.

those of **4a–f**[B(C₆F₅)₄]/**5a–f**[B(C₆F₅)₄]. As is evident from Scheme 4, this effect could be due to changes in $k_{\beta\text{-OR}}$ or $K_{5/4}$. However, the $K_{5/4}$ values that can be measured ($K_{5a/4a}$ and $K_{5b/4b}$) are very similar for the two anions, suggesting that the difference in $k_{\beta\text{-OR,obs}}$ values is due to the $k_{\beta\text{-OR}}$ term. This is likely to be true for the other vinyl ethers **2c–g**, as well. One possible explanation for the anion effect is that SbF₆[−], which is more strongly coordinating than B(C₆F₅)₄[−], may bind weakly to **4**, increasing the effective steric crowding and accelerating β -OR elimination.⁶⁰ This is consistent with the observation that sterically bulky α -diimine ligands promote β -OR elimination rate of the SbF₆[−] salts compared to B(C₆F₅)₄[−] salts of (α -diimine)PdCH₂CHMeOR⁺ and explains the anion effect on the product distribution in the multiple insertion reactions in Scheme 2.²¹

Conclusions

The Brookhart olefin polymerization catalyst (α -diimine)PdMe⁺ (**1**) reacts with vinyl ethers by two general pathways. First, **1** initiates the cationic polymerization of vinyl ethers **2a–c**. This pathway results in the decomposition of **1** to Pd⁰. Second, **1** reacts with stoichiometric quantities of **2a–g** by π complex formation, insertion, chain-walking, β -OR elimination, and allylic C–H activation to form (α -diimine)Pd(η^3 -C₃H₅)⁺ (**6**) and ROH. For silyl vinyl ethers **2d–f**, the β -OR elimination is sufficiently slow that up to three sequential vinyl ether insertions can occur prior to β -OR elimination.

The cationic vinyl ether polymerization and associated Pd⁰ formation and the β -OR elimination to form Pd allyl species that are unreactive for olefin insertion are catalyst deactivation processes that must be avoided in order to achieve **1**-catalyzed olefin/vinyl ether copolymerization. The copolymerization of 1-hexene with CH₂=CHOSiPh₃ (**2f**) by **1** is possible because insertion is much faster than cationic polymerization and β -OR elimination is relatively slow for this vinyl ether. However, the more electron-rich vinyl ethers **2a–c** are not suitable comonomers for **1** because for these substrates cationic polymerization out-competes insertion, and aryl vinyl ethers are unsuitable because β -OAr elimination is fast. The ability to strongly influence the reactivity of vinyl ethers with metal catalysts by modification of the vinyl ether structure, combined with the ability to tune catalyst behavior by modification of the ancillary ligands and anions, may enable broad use of vinyl ethers as comonomers in insertion polymerization of olefins.

Experimental Section

Methods and Materials. All manipulations were performed using drybox or Schlenk techniques under purified nitrogen or on a high-vacuum line unless indicated otherwise. Nitrogen was purified by passage through activated molecular sieves and Q-5 oxygen scavenger. Dichloromethane was dried over CaH₂, stored over P₂O₅, and freshly vacuum transferred prior to use. Tetrahydrofuran was distilled from sodium/benzophenone. Pentane, hexanes, toluene, and benzene were either distilled from sodium/benzophenone or purified by passage through activated alumina and BASF R3-11 oxygen removal catalyst. CD₂Cl₂ and CDCl₃ were degassed by three freeze–pump–thaw cycles and dried over P₂O₅.

2,6-Di-*tert*-butylpyridine was degassed by three freeze–pump–thaw cycles and distilled from CaH₂ under reduced pressure. (cod)PdCl₂ (cod = 1, 5-cyclooctadiene),⁶¹ (cod)PdMeCl,⁶² (α -diimine)PdMeCl (α -diimine = (2,6-(*i*-Pr)₂C₆H₃N=CMeCMe=N(2,6-(*i*-Pr)₂C₆H₃)),²² (α -diimine)PdMe(OEt₂)[SbF₆],^{22,63} [(η^3 -C₃H₅)Pd(μ -Cl)]₂,⁶⁴ and (tmeda)Pd(OPh)₂⁴³ were prepared by literature procedures. KOPh was synthesized by the reaction of KN(SiMe₃)₂ and phenol in THF and purified by washing with hexanes. [Li(Et₂O)_{*n*}][B(C₆F₅)₄] and [HNMe₂Ph][B(C₆F₅)₄] were obtained from Boulder Scientific. The Et₂O content in [Li(Et₂O)_{*n*}][B(C₆F₅)₄] was determined by ¹H NMR with C₆Me₆ as internal standard (*n* = 2.8). CH₂=CHO^{*t*}Bu, CH₂=CHOEt, and CH₂=CHOSiMe₃ were obtained from Aldrich, degassed by three freeze–pump–thaw cycles, and dried over CaH₂. CH₂=CHOSiMe₂Ph,⁶⁵ CH₂=CHOSiMePh₂,⁶⁵ CH₂=CHOSiPh₃,⁶⁵ and CH₂=CHOPh⁶⁶ were prepared using literature procedures. All other chemicals were purchased from Aldrich and used without further purification.

NMR spectra were recorded on Bruker DMX-500 or DRX-400 spectrometers in Teflon-valved tubes at 20 °C unless specified otherwise. ¹H and ¹³C chemical shifts are reported relative to SiMe₄ and were determined by reference to the residual solvent signals. Coupling constants are reported in hertz. For H₂C=CHX substrates, H_{cis} is the H that is cis to H_{int} and H_{trans} is the H that is trans to H_{int}. ¹³C NMR resonances were assigned with the assistance of DEPT-135 experiments. The NMR spectra of B(C₆F₅)₄[−] salts contain signals for the free B(C₆F₅)₄[−] anion. ¹³C{¹H} NMR (CD₂Cl₂): δ 148.5 (d, *J* = 242), 137.0 (d, *J* = 247), 135.6 (d, *J* = 244), 123.1 (br, C_{ipso}). ¹³C{¹H} NMR (CD₂Cl₂, −60 °C): δ 147.4 (d, *J* = 238), 137.7 (d, *J* = 244), 135.8 (d, *J* = 236), 123.2 (br, C_{ipso}). ¹⁹F NMR (CD₂Cl₂): δ −132.1 (br s, 8F, F_{ortho}), −161.3 (t, *J* = 20, 4F, F_{para}), −165.2 (t, *J* = 18, 8F, F_{meta}). ¹⁹F NMR (CD₂Cl₂, −70 °C): δ −132.5 (br s, 8F, F_{ortho}), −161.7 (t, *J* = 20, 4F, F_{para}), −164.9 (t, *J* = 18, 8F, F_{meta}). ¹¹B NMR (CD₂Cl₂): δ −16.1 (br s). ¹¹B NMR (CD₂Cl₂, −70 °C): δ −15.8 (br s).

Electrospray mass spectra (ESI-MS) were recorded on freshly prepared samples (ca. 1 mg/mL in CH₂Cl₂) using an Agilent 1100 LC-MSD spectrometer incorporating a quadrupole mass filter with an *m/z* range of 0–3000. Typical instrumental parameters included the following: drying gas temperature 350 °C, nebulizer pressure 35 psi, drying gas flow 12.0 L/min, and fragmentor voltage 0, 70, or 100 V. In all cases where assignments are given, the observed isotope patterns closely matched calculated isotope patterns. The listed *m/z* value corresponds to the most intense peak in the isotope pattern.

Polymerization of CH₂=CHO^{*t*}Bu (2a**) by 1[B(C₆F₅)₄].** An NMR tube was charged with (α -diimine)PdMeCl (13.6 mg, 0.0242 mmol), [Li(Et₂O)_{2.8}][B(C₆F₅)₄] (22.0 mg, 0.0246 mmol), and 2,6-di-*tert*-butylpyridine (9.2 mg, 0.048 mmol). CD₂Cl₂ (0.4 mL) and **2a** (0.68 mmol) were added by vacuum transfer at −196 °C. The tube was warmed to 20 °C, shaken vigorously, and monitored periodically by NMR. ¹H NMR spectra showed that −[CH₂CH(O^{*t*}Bu)]_{*n*}− had formed within 5 min, and **2a** was quantitatively converted to polymer after 20 h. Key NMR data for −[CH₂CH(O^{*t*}Bu)]_{*n*}−. ¹H NMR (CDCl₃): δ 9.70 (m, −CH₂CH(O^{*t*}Bu)CH₂C(=O)H), 5.53 (br, −CH₂CH(O^{*t*}Bu)CH=CHCH₂−), 5.40 (br, −CH₂CH(O^{*t*}Bu)CH=CHCH₂−), 4.90 (br m, −CH₂CH(O^{*t*}Bu)₂), 4.00 (br, −CH₂CH(O^{*t*}Bu)CH=CHCH₂−), 3.65 (CH₂CH(O^{*t*}Bu)−), 3.59 (br, −[CH₂CH(O^{*t*}Bu)]_{*n*}−), 2.35 (−CH₂CH(O^{*t*}Bu)CH=CHCH₂−), 1.63 (br, −[CH₂CH(O^{*t*}Bu)]_{*n*}−), 1.60 (−CH₂CH(O^{*t*}Bu)CH=CHCH₂−), 1.45 (−CH₂CH(O^{*t*}Bu)₂),

(61) Drew, D.; Doyle, J. R. *Inorg. Synth.* **1990**, 28, 348.

(62) Rülke, R. E. *Inorg. Chem.* **1993**, 32, 5769.

(63) McCord, E. F.; McLain, S. J.; Nelson, L. T. J.; Arthur, S. D.; Coughlin, E. B.; Ittel, S. D.; Johnson, L. K.; Tempel, D.; Killian, C. M.; Brookhart, M. *Macromolecules* **2001**, 34, 362.

(64) Tatsuno, Y.; Yoshida, T.; Otsuka, S. *Inorg. Synth.* **1990**, 28, 342.

(65) Schaumann, E.; Tries, F. *Synthesis* **2002**, 2, 191.

(66) Okimoto, Y.; Sakaguchi, S.; Ishii, Y. *J. Am. Chem. Soc.* **2002**, 124, 1590.

(60) (a) Macchioni, A.; Bellachioma, G.; Cardaci, G.; Travaglia, M.; Zuccaccia, C.; Milani, B.; Corso, G.; Zangrando, E.; Mestroni, G.; Carfagna, C.; Formica, M. *Organometallics* **1999**, 18, 3061. (b) Zuccaccia, C.; Macchioni, A.; Orabona, I.; Ruffo, F. *Organometallics* **1999**, 18, 4367. (c) Macchioni, A.; Magistrato, A.; Orabona, I.; Ruffo, F.; Rothlisberger, U.; Zuccaccia, C. *New J. Chem.* **2003**, 27, 455. (d) Macchioni, A. *Eur. J. Inorg. Chem.* **2003**, 195.

1.36 ($\text{CH}_3\text{CH}_2\text{CH}(\text{O}^t\text{Bu})-$), 1.19 (br, $-\text{[CH}_2\text{CH}(\text{O}^t\text{Bu})]_n-$), 1.10 ($\text{CH}_3\text{CH}(\text{O}^t\text{Bu})-$), 0.78 ($\text{CH}_3\text{CH}_2\text{CH}(\text{O}^t\text{Bu})-$). $^1\text{H}-^1\text{H}$ COSY correlations (CDCl_3): δ/δ 5.53 (br, $-\text{CH}_2\text{CH}(\text{O}^t\text{Bu})\text{CH}=\text{CHCH}_2-$)/2.35 ($-\text{CH}_2\text{CH}(\text{O}^t\text{Bu})\text{CH}=\text{CHCHH}'-$), 5.40 (br, $-\text{CH}_2\text{CH}(\text{O}^t\text{Bu})\text{CH}=\text{CHCH}_2-$)/4.00 (br, $-\text{CH}_2\text{CH}(\text{O}^t\text{Bu})\text{CH}=\text{CHCH}_2-$), 4.90 (br m, $-\text{CH}_2\text{CH}(\text{O}^t\text{Bu})_2$)/1.45 ($-\text{CH}_2\text{CH}(\text{O}^t\text{Bu})_2$), 3.65 ($\text{CH}_3\text{CH}(\text{O}^t\text{Bu})-$)/1.10 ($\text{CH}_3\text{CH}(\text{O}^t\text{Bu})-$), 3.59 (br, $-\text{[CH}_2\text{CH}(\text{O}^t\text{Bu})]_n-$)/1.63 (br, $-\text{[CH}_2\text{CH}(\text{O}^t\text{Bu})]_n-$), 1.36 ($\text{CH}_3\text{CH}_2\text{CH}(\text{O}^t\text{Bu})-$)/0.78 ($\text{CH}_3\text{CH}_2\text{CH}(\text{O}^t\text{Bu})-$). $^{13}\text{C}\{^1\text{H}\}$ NMR (CDCl_3): δ 73.2 (br, $-\text{CH}_2\text{CH}(\text{OCMe}_3)-$), 67.6 (br, *mm* $-\text{CH}_2\text{CH}(\text{O}^t\text{Bu})-$), 67.2 (br, *mr* $-\text{CH}_2\text{CH}(\text{O}^t\text{Bu})-$), 66.5 (br, *rr* $-\text{CH}_2\text{CH}(\text{O}^t\text{Bu})-$), 45.6 (br, $-\text{CH}_2\text{CH}(\text{O}^t\text{Bu})-$), 29.6 (br, $-\text{CH}_2\text{CH}(\text{OCMe}_3)-$); *mm*/*mr*/*rr* = 1:3:1.

Generation of $[(\alpha\text{-Diimine})\text{PdMe}(\text{CH}_2=\text{CHO}^t\text{Bu})][\text{SbF}_6]$ (3a** [**SbF₆**]).** An NMR tube was charged with **1** [**SbF₆**] (20.0 mg, 0.0237 mmol), and CD_2Cl_2 (0.4 mL) and **2a** (0.024 mmol) were added by vacuum transfer at -196°C . The tube was warmed to -78°C , shaken to dissolve and thoroughly mix the components, and placed in an NMR probe that had been precooled to -60°C . NMR spectra at -60°C showed that **3a** [**SbF₆**] (90%) had formed. ^1H NMR (CD_2Cl_2 , -60°C): δ 7.37–7.28 (m, 6H), 7.09 (dd, J = 13, 4, 1H, H_{int}), 3.27 (d, J = 13, 1H, H_{trans}), 2.96 (d, J = 4, 1H, H_{cis}), 2.92 (m, 1H, CHMe_2), 2.87 (m, 2H, CHMe_2), 2.72 (m, 1H, CHMe_2), 2.30 (s, 3H, $\text{N}=\text{CMe}$), 2.23 (s, 3H, $\text{N}=\text{CMe}$), 1.41 (d, J = 7, 3H, CHMe_2), 1.35 (s, 9H, OCMe_3), 1.32 (d, J = 7, 3H, CHMe_2), 1.26 (d, J = 7, 3H, CHMe_2), 1.24 (d, J = 7, 3H, CHMe_2), 1.16 (d, J = 7, 3H, CHMe_2), 1.15 (d, J = 7, 3H, CHMe_2), 1.14 (d, J = 7, 3H, CHMe_2), 1.08 (d, J = 7, 3H, CHMe_2), 0.14 (s, 3H, PdMe). $^{13}\text{C}\{^1\text{H}\}$ NMR (CD_2Cl_2 , -60°C): δ 179.3 ($\text{N}=\text{CMe}$), 175.3 ($\text{N}=\text{CMe}$), 148.2 ($\text{CH}_2=\text{CHO}^t\text{Bu}$), 139.4, 139.0, 138.2, 137.8, 137.6, 137.1, 128.09, 128.06, 124.65, 124.62, 124.13, 124.11, 83.6 (OCMe_3), 54.4 ($\text{CH}_2=\text{CHO}^t\text{Bu}$), 28.8, 28.6, 28.41, 28.36, 27.5, 24.4, 24.0 (2C), 23.9, 23.5, 23.4, 22.9, 22.8, 21.6, 16.7 (PdMe).

Generation of $[(\alpha\text{-Diimine})\text{PdMe}(\text{CH}_2=\text{CHO}^t\text{Bu})][\text{B}(\text{C}_6\text{F}_5)_4]$ (3a** [**B(C₆F₅)₄**]).** An NMR tube was charged with $(\alpha\text{-diimine})\text{PdMeCl}$ (12.0 mg, 0.0214 mmol) and $[\text{Li}(\text{Et}_2\text{O})_{2.8}][\text{B}(\text{C}_6\text{F}_5)_4]$ (20.2 mg, 0.0226 mmol). CD_2Cl_2 (0.4 mL) was added by vacuum transfer at -196°C . The tube was warmed to 20°C and shaken for 10 min. **2a** (0.04 mmol) was added by vacuum transfer at -196°C . The tube was kept at 0°C for 10 min. The volatiles were evacuated, and CD_2Cl_2 (0.4 mL) was added by vacuum transfer at -196°C . The tube was warmed to 20°C , shaken vigorously, and monitored periodically by NMR. NMR analysis showed a mixture of $\{[(\alpha\text{-diimine})\text{PdMe}]_2(\mu\text{-Cl})\}^+$ (8%), **3a** [**B(C₆F₅)₄**] (78%), $[(\alpha\text{-diimine})\text{Pd}\{\text{CH}_2\text{CHMe}(\text{O}^t\text{Bu})\}][\text{B}(\text{C}_6\text{F}_5)_4]$ (**4a** [**B(C₆F₅)₄**], 10%), and $[(\alpha\text{-diimine})\text{Pd}\{\text{CMe}_2(\text{O}^t\text{Bu})\}][\text{B}(\text{C}_6\text{F}_5)_4]$ (**5a** [**B(C₆F₅)₄**], 4%) after 10 min. The NMR spectra of **3a** [**B(C₆F₅)₄**] are very similar to those of **3a** [**SbF₆**].

Generation of **4a [**B(C₆F₅)₄**] and **5a** [**B(C₆F₅)₄**].** An NMR tube was charged with $(\alpha\text{-diimine})\text{PdMeCl}$ (12.0 mg, 0.0214 mmol) and $[\text{Li}(\text{Et}_2\text{O})_{2.8}][\text{B}(\text{C}_6\text{F}_5)_4]$ (20.2 mg, 0.0226 mmol). CD_2Cl_2 (0.4 mL) was added by vacuum transfer at -196°C . The tube was warmed to 20°C and shaken for 10 min. **2a** (0.04 mmol) was added by vacuum transfer at -196°C . The tube was kept at 0°C for 10 min. The volatiles were evacuated, and CD_2Cl_2 (0.4 mL) was added by vacuum transfer at -196°C . The tube was warmed to 20°C , shaken vigorously, and monitored periodically by NMR. NMR analysis showed that, after 2 h, a mixture of **3a** [**B(C₆F₅)₄**] (3%), **4a** [**B(C₆F₅)₄**] (66%), and **5a** [**B(C₆F₅)₄**] (25%) was present. After

22 h, the consumption of **3a** [**B(C₆F₅)₄**] was complete, and **4a** [**B(C₆F₅)₄**] (59%), **5a** [**B(C₆F₅)₄**] (22%), and $[(\alpha\text{-diimine})\text{Pd}(\eta^3\text{-C}_3\text{H}_5)][\text{B}(\text{C}_6\text{F}_5)_4]$ (**6** [**B(C₆F₅)₄**], 16%) were present. ESI-MS of $(\alpha\text{-diimine})\text{Pd}\{\text{CH}_2\text{CH}(\text{O}^t\text{Bu})\text{Me}\}^+$ and $(\alpha\text{-diimine})\text{Pd}\{\text{CMe}_2(\text{O}^t\text{Bu})\}^+$: calcd m/z = 625.3, found 625.2. The aromatic ^1H NMR resonances of **4a** [**B(C₆F₅)₄**] and **5a** [**B(C₆F₅)₄**] overlap, and the ^{13}C NMR resonances of these species are very similar and therefore only key NMR data are listed.⁶⁷ Key NMR data for **4a** [**B(C₆F₅)₄**]. ^1H NMR (CD_2Cl_2): δ 4.86 (m, 1H, $\text{PdCH}_2\text{CHMe}(\text{O}^t\text{Bu})$), 3.79 (sept, J = 7, 1H, CHMe_2), 3.29 (sept, J = 7, 1H, CHMe_2), 2.93 (sept, J = 7, 1H, CHMe_2), 2.61 (sept, J = 7, 1H, CHMe_2), 2.20 (s, 3H, $\text{N}=\text{CMe}$), 2.17 (s, 3H, $\text{N}=\text{CMe}$), 0.93 (t, J = 7, 1H, $\text{PdCHH}'\text{CHMe}(\text{O}^t\text{Bu})$), 0.85 (s, 9H, OCMe_3), 0.40 (dd, J = 7, 4, 1H, $\text{PdCHH}'\text{CHMe}(\text{O}^t\text{Bu})$). The $\text{PdCH}_2\text{CHMe}(\text{O}^t\text{Bu})$ signal is obscured but was identified by COSY NMR at δ 1.22. $^1\text{H}-^1\text{H}$ COSY correlations (CD_2Cl_2 , -40°C): δ/δ 4.83 ($\text{PdCH}_2\text{CHMe}(\text{O}^t\text{Bu})$)/1.22 ($\text{PdCH}_2\text{CHMe}(\text{O}^t\text{Bu})$), 4.83 ($\text{PdCH}_2\text{CHMe}(\text{O}^t\text{Bu})$)/0.81 ($\text{PdCHH}'\text{CHMe}(\text{O}^t\text{Bu})$), 4.83 ($\text{PdCH}_2\text{CHMe}(\text{O}^t\text{Bu})$)/0.27 ($\text{PdCHH}'\text{CHMe}(\text{O}^t\text{Bu})$), 0.81 ($\text{PdCHH}'\text{CHMe}(\text{O}^t\text{Bu})$)/0.27 ($\text{PdCHH}'\text{CHMe}(\text{O}^t\text{Bu})$). ^1H NMR (CDCl_2F , -130°C): δ 4.85 (m, 1H, $\text{PdCH}_2\text{CHMe}(\text{O}^t\text{Bu})$), 3.96 (m, J = 7, 1H, CHMe_2), 3.32 (sept, J = 7, 1H, CHMe_2), 2.84 (sept, J = 7, 1H, CHMe_2), 2.46 (sept, J = 7, 1H, CHMe_2), 0.78 (s, 9H, OCMe_3). $^{13}\text{C}\{^1\text{H}\}$ NMR (CD_2Cl_2 , -40°C): δ 88.9 (OCMe_3), 88.3 ($\text{PdCH}_2\text{CHMe}(\text{O}^t\text{Bu})$), 9.3 ($\text{PdCH}_2\text{CHMe}(\text{O}^t\text{Bu})$). Key NMR data for **5a** [**B(C₆F₅)₄**]. ^1H NMR (CD_2Cl_2): δ 3.05 (sept, J = 7, 4H, CHMe_2), 2.21 (s, 3H, $\text{N}=\text{CMe}$), 2.20 (s, 3H, $\text{N}=\text{CMe}$), 1.11 (s, 9H, OCMe_3), 0.64 (s, 6H, $\text{PdCMe}_2(\text{O}^t\text{Bu})$). ^1H NMR (CDCl_2F , -130°C): δ 3.02 (sept, J = 7, 4H, CHMe_2), 1.07 (s, 9H, OCMe_3), 0.63 (s, 6H, CMe_2). $^{13}\text{C}\{^1\text{H}\}$ NMR (CD_2Cl_2 , -40°C): δ 90.3 (OCMe_3), 82.8 ($\text{PdCMe}_2(\text{O}^t\text{Bu})$).

The first-order rate constant for the consumption of **3a** [**B(C₆F₅)₄**] ($k_{\text{insert}, 3a}$) was measured by the disappearance of the PdMe resonance of **3a** [**B(C₆F₅)₄**] and increase of the PdCH_2CHMe resonance of **4a** [**B(C₆F₅)₄**] plus the PdCMe_2 resonance of **5a** [**B(C₆F₅)₄**]. The equilibrium constant $K_{5/4}$ was determined from the ratio of the integrated intensities of the PdCMe_2 resonance of **5a** [**B(C₆F₅)₄**] and the PdCH_2CHMe resonance of **4a** [**B(C₆F₅)₄**].

Reaction of **4a [**B(C₆F₅)₄**]/**5a** [**B(C₆F₅)₄**] with MeCN.** An NMR tube containing a CD_2Cl_2 solution (0.4 mL) of **4a** [**B(C₆F₅)₄**] (0.016 mmol) and **5a** [**B(C₆F₅)₄**] (0.0055 mmol) was frozen at -196°C , and MeCN (0.026 mmol) was added by vacuum transfer. The tube was warmed to -78°C , agitated to mix the components, placed in an NMR probe that had been precooled to -60°C , and monitored by NMR. ^1H NMR spectra showed that, after 5 min, **4a** [**B(C₆F₅)₄**] had been consumed, and a mixture of **5a** [**B(C₆F₅)₄**] (24%) and **4a-MeCN** [**B(C₆F₅)₄**] (76%) was present. The tube was then warmed to -40°C and monitored periodically by NMR. After 140 min, a mixture of **5a** [**B(C₆F₅)₄**] (5%) and **4a-MeCN** [**B(C₆F₅)₄**] (91%) was present. Exchange between free and coordinated MeCN is slow on the NMR time scale at -40°C . Compound **4a** [**B(C₆F₅)₄**] was not detected during this reaction. Data for **4a-MeCN** [**B(C₆F₅)₄**]. ^1H NMR (CD_2Cl_2 , -40°C): δ 7.42–7.26 (m, 6H), 3.18 (m, 1H, $\text{PdCH}_2\text{CHMe}(\text{O}^t\text{Bu})$), 2.90 (m, 2H, CHMe_2), 2.83 (m, 2H, CHMe_2), 2.21 (s, 3H, $\text{N}=\text{CMe}$), 2.19 (s, 3H, $\text{N}=\text{CMe}$), 1.71 (s, 3H, MeCN), 1.53 (m, 1H, $\text{PdCHH}'\text{CHMe}(\text{O}^t\text{Bu})$), 1.31 (d, J = 6, 12H, CHMe_2), 1.15 (d, J = 6, 6H, CHMe_2), 1.10 (3H, CHMe_2), 1.08 (3H, CHMe_2), 0.97 (d, J = 6, 3H, $\text{PdCH}_2\text{CHMe}(\text{O}^t\text{Bu})$), 0.84 (s, 9H, OCMe_3). The other PdCHH' signal is obscured but was identified by COSY NMR at δ 1.15. Key $^1\text{H}-^1\text{H}$ COSY correlations (CD_2Cl_2 , -40°C , NMR 500–2, 45–126) δ/δ : 3.18 ($\text{PdCH}_2\text{CHMe}(\text{O}^t\text{Bu})$)/1.53 ($\text{PdCHH}'\text{CHMe}(\text{O}^t\text{Bu})$), 3.18 ($\text{PdCH}_2\text{CHMe}(\text{O}^t\text{Bu})$)/1.15 ($\text{PdCHH}'\text{CHMe}(\text{O}^t\text{Bu})$), 3.18 ($\text{PdCH}_2\text{CHMe}(\text{O}^t\text{Bu})$)/0.97 ($\text{PdCH}_2\text{CHMe}(\text{O}^t\text{Bu})$), 1.53 ($\text{PdCHH}'\text{CHMe}(\text{O}^t\text{Bu})$)/1.15 ($\text{PdCHH}'\text{CHMe}(\text{O}^t\text{Bu})$). $^{13}\text{C}\{^1\text{H}\}$ NMR (CD_2Cl_2 , -40°C): δ 179.8 ($\text{N}=\text{CMe}$), 172.1 ($\text{N}=\text{CMe}$), 139.7, 139.4, 138.4, 138.2, 137.4 (2C), 128.9, 128.1, 124.7, 124.6, 124.1, 124.0, 121.8, 72.8 (OCMe_3), 67.2 ($\text{PdCH}_2\text{CHMe}(\text{O}^t\text{Bu})$), 36.9 ($\text{PdCH}_2\text{CHMe}(\text{O}^t\text{Bu})$), 28.95, 28.92, 28.7, 28.6, 27.8, 25.6, 23.8, 23.6, 23.3, 23.2, 23.1, 23.0 (2C), 22.8, 22.2, 20.0, 2.0 (MeCN).

(67) $^{13}\text{C}\{^1\text{H}\}$ NMR of $[(\alpha\text{-diimine})\text{Pd}\{\text{CH}_2\text{CHMe}(\text{O}^t\text{Bu})\}][\text{B}(\text{C}_6\text{F}_5)_4]$ and $[(\alpha\text{-diimine})\text{Pd}\{\text{CMe}_2(\text{O}^t\text{Bu})\}][\text{B}(\text{C}_6\text{F}_5)_4]$: δ 178.1, 174.5, 171.6, 143.4, 142.8, 141.6, 140.9, 138.5, 137.8, 137.5, 137.0, 136.5, 136.2, 128.7, 128.1, 127.9, 127.6, 124.54, 124.48, 124.41, 124.36 (2C), 124.2, 90.3, 88.9, 88.3, 82.9, 30.6, 29.7, 29.04, 28.99, 28.95, 28.75, 28.65, 28.6, 26.2, 25.5, 24.5, 24.0, 23.8, 23.7, 23.29, 23.25, 22.9, 22.8, 22.6, 22.5, 22.3, 21.2, 21.1, 20.0, 19.5, 9.3. One of the $\text{N}=\text{CMe}$ resonances of $[(\alpha\text{-diimine})\text{Pd}\{\text{CMe}_2(\text{O}^t\text{Bu})\}][\text{B}(\text{C}_6\text{F}_5)_4]$ was obscured, and the OCMe_3 resonances for $[(\alpha\text{-diimine})\text{Pd}\{\text{CH}_2\text{CHMe}(\text{O}^t\text{Bu})\}][\text{B}(\text{C}_6\text{F}_5)_4]$ and $[(\alpha\text{-diimine})\text{Pd}\{\text{CMe}_2(\text{O}^t\text{Bu})\}][\text{B}(\text{C}_6\text{F}_5)_4]$ overlap.

Conversion of 4a[B(C₆F₅)₄]/5a[B(C₆F₅)₄] to 6[B(C₆F₅)₄]. An NMR tube containing a CD₂Cl₂ solution of **4a**[B(C₆F₅)₄] (0.038 mmol) and **5a**[B(C₆F₅)₄] (0.014 mmol) was maintained at 20 °C and monitored by NMR periodically. Over the course of 15 days, 90% of **4a**[B(C₆F₅)₄] and **5a**[B(C₆F₅)₄] were converted to **6**[B(C₆F₅)₄] and HO^tBu. The first-order rate constant for consumption of the total of **4a**[B(C₆F₅)₄] and **5a**[B(C₆F₅)₄] was measured by the disappearance of the sum of the PdCH₂CHMe resonance of **4a**[B(C₆F₅)₄] and the PdCMe₂ resonance of **5a**[B(C₆F₅)₄]. **6**[B(C₆F₅)₄] was prepared by the procedure reported by Risse for the analogous compound [(2,2'-bipyridyl)Pd(η³-C₃H₅)] [SbF₆] and characterized by X-ray diffraction (see Supporting Information).⁶⁸ NMR data for **6**[B(C₆F₅)₄]. ¹H NMR (CD₂Cl₂): δ 7.41–7.32 (m, 6H), 5.65 (m, 1H, H_{int}), 3.36 (d, *J* = 7, 2H, H_{syn}), 3.04 (d, *J* = 13, 2H, H_{anti}), 2.96 (sept, *J* = 7, 2H, CHMe₂), 2.70 (sept, *J* = 7, 2H, CHMe₂), 2.26 (s, 6H, N=CMe), 1.35 (d, *J* = 7, 6H, CHMe₂), 1.26 (d, *J* = 7, 6H, CHMe₂), 1.23 (d, *J* = 7, 6H, CHMe₂), 1.21 (d, *J* = 7, 6H, CHMe₂). ¹³C{¹H} NMR (CD₂Cl₂): δ 176.9 (N=CMe), 144.0, 137.1, 137.0, 129.1, 125.0, 125.0, 121.1, 65.8 (allyl CH₂), 29.8, 29.5, 23.7, 23.6, 23.4, 23.3, 20.1. ESI-MS of (α-diimine)Pd(η³-C₃H₅)⁺: calcd *m/z* = 551.3, found 551.2. Anal. Calcd for C₅₅H₄₅BF₂₀N₂Pd: C, 53.66; H, 3.68; N, 2.28. Found: C, 53.78; H, 3.67; N, 2.19.

The first-order rate constant for consumption of the total of **4a**[B(C₆F₅)₄] and **5a**[B(C₆F₅)₄], *k*_{β-O^tBu,obs}, was measured by the disappearance of the PdCH₂CHMe ¹H NMR resonance of **4a**[B(C₆F₅)₄] plus the PdCMe₂ ¹H NMR resonance of **5a**[B(C₆F₅)₄] and the increase in the H_{int} resonance of **6**[B(C₆F₅)₄].

Insertion of 3a[SbF₆] and Reactions of 1 with 2b–g. The insertion rate constant of **3a**[SbF₆], the equilibrium constant between **5a**[SbF₆] and **4a**[SbF₆], and the β-O^tBu elimination rate constant of **5a**[SbF₆]/**4a**[SbF₆] were measured by the methods described above for the B(C₆F₅)₄[−] salts. The reactions of **1**[SbF₆] and **1**[B(C₆F₅)₄] with **2b–g** were studied using the procedures described above for **2a**. Full details are provided in the Supporting Information.

Competitive Binding of Ethylene and CH₂=CHOR (2a–c) to 1[SbF₆] (eq 4). The procedure for **2a** is described here; an identical procedure was used for **2b,c**. An NMR tube was charged with **1**[SbF₆] (15.0 mg, 0.0179 mmol). CD₂Cl₂ (0.4 mL) was added by vacuum transfer at −196 °C. The tube was warmed to 20 °C and shaken. Ethylene (0.062 mmol) and **2a** (0.040 mmol) were added by vacuum transfer at −196 °C. The tube was warmed to −78 °C, shaken, and placed in an NMR probe that had been precooled to −60 °C. The reaction was monitored periodically by ¹H NMR at −60 °C until the reaction quotient *Q*_{2a/ethylene} = [**3a**][CH₂=CH₂]/[(α-diimine)PdMe(CH₂=CH₂)⁺]^{−1}[**2a**]^{−1} reached a constant value. Additional **2a** (0.062 mmol) was added by vacuum transfer to change the ethylene/**2a** ratio, and the tube was monitored by ¹H NMR at −60 °C until *Q*_{2a/ethylene} again reached a constant value. This process was repeated one more time, and the average *K*_{2a/ethylene} (SbF₆[−]) value is reported in Table 2. The competitive binding of **2d–g** and **2c** to **1**[SbF₆] at −20 °C (eq 5) and of ethylene and CH₂=CHOR (**2a–c**, **2g**) to **1**[B(C₆F₅)₄] at −60 °C (eq 4) was studied in a similar manner.

Generation of [(tmeda)Pd(OPh)]_n[B(C₆F₅)₄]_n (7**).** An NMR tube was charged with (tmeda)Pd(OPh)₂ (10.9 mg, 0.0267 mmol), [HNMe₂Ph][B(C₆F₅)₄] (21.6 mg, 0.0270 mmol), and CD₂Cl₂ (0.4 mL) was added by vacuum transfer at −196 °C. The tube was warmed to 20 °C and shaken vigorously. NMR spectra showed that [(tmeda)Pd(OPh)]_n[B(C₆F₅)₄]_n, NMe₂Ph, and HOPh had formed quantitatively in 10 min.⁶⁹ The ESI-MS contains signals for only the mononuclear monocation (tmeda)Pd(OPh)⁺ even at

low fragmentor voltage, while ¹H PGSE NMR experiments suggest a tetrameric structure (*n* = 4), referencing [(tmeda)Pd(OPh)(NCMe)][B(C₆F₅)₄] as a monomeric analogue.⁷⁰ These results indicate that **7** is most likely a labile oligomer in CD₂Cl₂ solution. Key NMR data for **7**. ¹H NMR (CD₂Cl₂): δ 7.73 (d, *J* = 8, 2H, H_{ortho}), 7.45 (t, *J* = 8, 2H, H_{meta}), 7.27 (t, *J* = 8, 1H, H_{para}), 2.46 (m, 4H, −CH₂−), 2.08 (s, 12H, NMe₂). ¹³C{¹H} NMR (CD₂Cl₂): δ 158.8, 131.8, 126.1, 124.3, 64.0, 50.6. ESI-MS of (tmeda)Pd(OPh)⁺: calcd *m/z* = 315.1, found 315.0.

Reaction of 7 with Propylene. The above solution of in situ generated **7** was frozen at −196 °C, and propylene (1 equiv) was added by vacuum transfer. The tube was warmed to −30 °C. ¹H NMR showed no reaction occurred after 30 min at −30 °C. The sample was then warmed to 20 °C. After 10 h, ¹H NMR showed that **7** was completely converted to [(tmeda)Pd(η³-C₃H₅)] [B(C₆F₅)₄] and HOPh.

[(tmeda)Pd(OPh)(NCMe)][B(C₆F₅)₄] ([7-MeCN])[B(C₆F₅)₄]. A solution of in situ generated **7** in CD₂Cl₂ was frozen at −196 °C, and MeCN (1.1 equiv) was added by vacuum transfer. The tube was warmed to 20 °C and shaken. ¹H NMR showed that [7-MeCN][B(C₆F₅)₄] had formed quantitatively in 5 min. ¹H NMR (CD₂Cl₂): δ 7.11–7.06 (m, 4H), 6.69 (m, 1H, H_{para}), 2.78 (m, 2H, −CH₂−), 2.72 (s, 6H, NMe₂), 2.68 (s, 6H, NMe₂), 2.55 (m, 2H, −CH₂−), 2.08 (MeCN). ¹³C{¹H} NMR (CD₂Cl₂): δ 165.9, 156.4, 129.6, 119.8, 117.2, 63.3, 62.3, 51.7, 50.9, 3.1 (MeCN). ESI-MS of (tmeda)Pd(OPh)(NCMe)⁺: calcd *m/z* = 356.1, found 356.0.⁷¹

[(tmeda)Pd(η³-C₃H₅)] [B(C₆F₅)₄]. This species was prepared following the procedure reported by Risse for the analogous compound [(2,2'-bipyridyl)Pd(η³-C₃H₅)] [SbF₆].⁷² ¹H NMR (CD₂Cl₂): δ 5.66 (m, 1H, H_{int}), 3.79 (d, *J* = 7, 2H, H_{syn}), 3.00 (d, *J* = 13, 2H, H_{anti}), 2.91 (s, 6H, NMe₂), 2.73 (s, 6H, NMe₂), 2.80 (m, 2H, −CH₂−), 2.71 (m, 2H, −CH₂−). ¹³C{¹H} NMR (CD₂Cl₂): δ 119.8 (allyl CH), 61.9, 61.1, 52.5 (NMe₂), 51.9 (NMe₂). ESI-MS of (tmeda)Pd(η³-C₃H₅)⁺: calcd *m/z* = 263.1, found 263.0. Anal. Calcd for C₃₃H₂₁BF₂₀N₂Pd: C, 42.04; H, 2.25; N, 2.97. Found: C, 42.13; H, 2.31; N, 2.89.

Computational Methods. DFT computations were performed using Gaussian 03.⁷³ The geometries of the stationary points were found using the B3LYP functional.⁷⁴ C, H, N, and O atoms were modeled using the 6-31G* basis set,⁷⁵ and Pd and Si were modeled using the LANL2DZ basis set including the relativistic pseudopotentials of Hay and Wadt.⁷⁶

Acknowledgment. This work was supported by the U.S. Department of Energy (DE-FG-02-00ER15036).

Supporting Information Available: Experimental procedures, characterization of complexes, details of kinetic studies, and complete ref 73. This material is available free of charge via the Internet at <http://pubs.acs.org>.

JA100491Y

- (68) (a) Rush, S.; Reinmuth, A.; Risse, W. *Macromolecules* **1997**, *30*, 7375. (b) For [(α-diimine)Pd(η³-C₃H₅)] [3,5-(CF₃)₂C₆H₃]] see: Li, W.; Zhang, X.; Meetsma, A.; Hessen, B. *J. Am. Chem. Soc.* **2004**, *126*, 12246. (69) NMR spectra showed that NMe₂Ph and HOPh are both free and do not coordinate to the [(tmeda)Pd(OPh)]_n[B(C₆F₅)₄]_n in CD₂Cl₂ at 20 °C.

- (70) For the related tetrameric compound [(cod)₄Pt₄(μ²-OH)₄](OTf)₄, see: Szuromi, E. Ph.D. Thesis, University of Missouri—Columbia, December 2005. (71) The major peak is (tmeda)Pd(OPh)⁺ calcd. *m/z* = 315.1, found 315.0. (72) For the related compound [(tmeda)Pd(η³-C₃H₅)]Br, see: Graff, W.; Boersma, J.; Koten, G. *Organometallics* **1990**, *9*, 1479. (73) Frisch, M. J.; et al. *Gaussian 03*, revision C.02; Gaussian, Inc.: Wallingford, CT, 2004. See the Supporting Information for the complete citation. (74) (a) Becke, A. D. *J. Chem. Phys.* **1993**, *98*, 5648. (b) Lee, C.; Yang, W.; Parr, R. G. *Phys. Rev. B* **1988**, *37*, 785. (c) Miehlich, B.; Savin, A.; Stoll, H.; Preuss, H. *Chem. Phys. Lett.* **1989**, *157*, 200. (75) (a) Rassolov, V. A.; Ratner, M. A.; Pople, J. A.; Redfern, P. C.; Curtiss, L. A. *J. Comput. Chem.* **2001**, *22*, 976. (b) Rassolov, V. A.; Pople, J. A.; Ratner, M. A.; Windus, T. L. *J. Chem. Phys.* **1998**, *109*, 1223. (c) Ditchfield, R.; Hehre, W. J.; Pople, J. A. *J. Chem. Phys.* **1971**, *54*, 724. (76) (a) Hay, P. J.; Wadt, W. R. *J. Chem. Phys.* **1985**, *82*, 270. (b) Wadt, W. R.; Hay, P. J. *J. Chem. Phys.* **1985**, *82*, 284. (c) Hay, P. J.; Wadt, W. R. *J. Chem. Phys.* **1985**, *82*, 299.